Received: 19 July 2018 | Revised: 8 November 2018 | Accepted: 13 November 2018
DOI: 10.1002/glia.23574

GLIA
WILEY

RESEARCH ARTICLE

Extracellular ATP and glutamate drive pyruvate production and energy demand to regulate mitochondrial respiration in astrocytes

Inés Juaristi[1,2,3] | Irene Llorente-Folch[4,5] | Jorgina Satrústegui[1,2,3] | Araceli del Arco[2,3,6]

[1]Departamento de Biología Molecular, Centro de Biología Molecular Severo Ochoa, Consejo Superior de Investigaciones Científicas-Universidad Autónoma de Madrid (CSIC-UAM), Madrid, Spain

[2]Centro de Investigación Biomédica en Red de Enfermedades Raras (CIBERER), Madrid, Spain

[3]Instituto de Investigación Sanitaria Fundación Jiménez Díaz (IIS-FJD), Madrid, Spain

[4]Department of Physiology & Medical Physics, Royal College of Surgeons in Ireland, Dublin, Ireland

[5]Center for Systems Medicine, Royal College of Surgeons in Ireland, Dublin, Ireland

[6]Facultad de Ciencias Ambientales y Bioquímica, Centro Regional de Investigaciones Biomédicas, Universidad de Castilla la Mancha, Toledo, Spain

Correspondence
Jorgina Satrústegui, PhD, Departamento de Biología Molecular, Centro de Biología Molecular Severo Ochoa, Consejo Superior de Investigaciones Científicas-Universidad Autónoma de Madrid (CSIC-UAM), Nicolás Cabrera, 1, 28049 Madrid, Spain.
Email: jsatrustegui@cbm.csic.es

Funding information
Fundación Ramón Areces; Instituto de Salud Carlos III; Fundación Ramón Areces; Ministerio de Economía, Grant/Award Numbers: SAF2017-82560-R, SAF2014-56929R

Abstract

Astrocytes respond to energetic demands by upregulating glycolysis, lactate production, and respiration. This study addresses the role of respiration and calcium regulation of respiration as part of the astrocyte response to the workloads caused by extracellular ATP and glutamate. Extracellular ATP (100 μM to 1 mM) causes a Ca^{2+}-dependent workload and fall of the cytosolic ATP/ADP ratio which acutely increases astrocytes respiration. Part of this increase is related to a Ca^{2+}-dependent upregulation of cytosolic pyruvate production. Conversely, glutamate (200 μM) causes a Na^{+}, but not Ca^{2+}, dependent workload even though glutamate-induced Ca^{2+} signals readily reach mitochondria. The glutamate workload triggers a rapid fall in the cytosolic ATP/ADP ratio and stimulation of respiration. These effects are mimicked by D-aspartate a non-metabolized agonist of the glutamate transporter, but not by a metabotropic glutamate receptor agonist, indicating a major role of Na^{+}-dependent workload in stimulated respiration. Glutamate-induced increase in respiration is linked to a rapid increase in glycolytic pyruvate production, suggesting that both glutamate and extracellular ATP cause an increase in astrocyte respiration fueled by workload-induced increase in pyruvate production. However, glutamate-induced pyruvate production is partly resistant to glycolysis blockers (iodoacetate), indicating that oxidative consumption of glutamate also contributes to stimulated respiration. As stimulation of respiration by ATP and glutamate are similar and pyruvate production smaller in the first case, the results suggest that the response to extracellular ATP is a Ca^{2+}-dependent upregulation of respiration added to glycolysis upregulation. The global contribution of astrocyte respiratory responses to brain oxygen consumption is an open question.

KEYWORDS

astrocytes, ATP, calcium, glutamate, pyruvate, respiration, workload

1 | INTRODUCTION

Increases in calcium concentration switch on the activity of most cells, particularly excitable cells. Increases in cell activity cause ATP breakdown which is restored by an upregulation of ATP production in the cytosol or mitochondria. Calcium parallel activation of ATP utilization and production pathways has been proposed to play a key role in the maintenance of energetic homeostasis (Glancy, Willis, Chess, & Balaban, 2013). Calcium may activate ATP production via upregulation of oxidative phosphorylation (OXPHOS), a process known for a long time and largely attributed to calcium entry in mitochondria through the calcium uniporter, MCU, and activation of matrix dehydrogenases and other transporters or enzymes. However, calcium regulation of ATP production is not limited to MCU-dependent effects. For example, in neurons, calcium activates the malate aspartate NADH shuttle (MAS) through Aralar/AGC1/Slc25a12, a calcium regulated mitochondrial aspartate–glutamate transporter with calcium binding motifs facing the intermembrane space (Palmieri et al., 2001), critical to transfer reducing equivalents to mitochondria (Pardo et al., 2006; Satrústegui, Pardo, & Del Arco, 2007), to maintain basal respiration and to provide a Ca^{2+}-boost to workload stimulated respiration (Llorente-Folch et al., 2013, 2015; Rueda et al., 2014). The mitochondrial ATP-Mg/Pi carrier

SCaMC-3/Slc25a23 with Ca^{2+} binding motifs also facing the intermembrane space (Del Arco & Satrústegui, 2004; Fiermonte et al., 2004) has been shown to play a role in maintaining respiration and mitochondrial ATP levels in response to NMDA-dependent PARP-1 stimulation in neurons (Rueda et al., 2015). Moreover, in addition to effects in mitochondria, Ca^{2+} may stimulate glycogenolysis, glycolysis, and glucose transport, particularly in astrocytes (Hertz et al., 2015; Müller, Fox, Schousboe, Waagepetersen, & Bak, 2014; Porras, Ruminot, Loaiza, & Barros, 2008) and in this way increase substrate supply to mitochondria.

The present study was aimed at analyzing the role of calcium in workload-stimulation of cell respiration in astrocytes. The characteristics of brain astrocyte glucose metabolism (Nortley & Attwell, 2017) and the relative roles of respiration and lactate production in astrocytes, particularly after stimulation conditions, are currently debated. The small size of astrocyte mitochondria, the absence of immunolabeling with anti-cytochrome oxidase antibodies (Wong-Riley, Trusk, Tripathi, & Hoppe, 1989) and the extremely small diameter of astrocyte processes, have led to the belief that mitochondrial function in astrocytes is not critical in terms of energy production. However, mitochondria are present even in these processes (Jackson & Robinson, 2018; Stephen et al., 2015), and calculations from *in vivo* NMR spectroscopy indicate that about 30% of brain oxidative metabolism takes place in astrocytes (Hertz, Peng, & Dienel, 2007).

The gold standard for mitochondrial function is respirometry and this requires a homogeneous cell population to assign variations in oxygen consumption rate (OCR) to a given cell type. Isolation of single cell types in brain can be performed by laser microdissection or fluorescence-activated cell sorting of labeled cells, but CNS-derived cells are highly branched and interconnected, and these isolations lead to the loss of the most distant and connected cellular structures. The proteomic information obtained from these cells may not be accurate. Primary cell culture allows the isolation of entire cells, but may affect the expression pattern of some of the proteins. However, although cultured astrocytes are different than astrocytes acutely isolated from brain (Cahoy et al., 2008) a recent proteomic study in cultured and acutely isolated brain astrocytes revealed that these differences were not so large, and involved mainly increases in proteins from the extracellular matrix in cultured astrocytes (Sharma et al., 2015). Therefore, we have used cultured astrocytes to study of the respiratory responses to relevant agonists (ATP and glutamate) released by activated neurons and by astrocytes through P2X7 and connexin hemichannels (Covelo & Araque, 2018, Parpura et al., 2017). We have specifically addressed the type of workloads imposed on astrocytes by these agonists and the role of calcium in the final respiratory response.

We have found that extracellular ATP produced a substantial stimulation of respiration which was clearly calcium sensitive. Interestingly, a main contributor to this Ca^{2+}-sensitive increase was not mitochondrial in origin. It resulted from a rapid increase in cytosolic pyruvate arising from Ca^{2+}-stimulation of glycolysis. On the other hand, Ca^{2+} regulation did not contribute to the increase in respiration produced by activation of excitatory neurotransmitter uptake (glutamate or D-aspartate) which was linked to an upregulation of glycolytic pyruvate production.

2 | MATERIALS AND METHODS

2.1 | Animals

SVJ129-C57BL/6 wild-type mice without distinction of gender were used. Mice were housed in a humidity- and temperature-controlled room on a 12-hr light/dark cycle, receiving water and food ad libitum. All animal procedures were approved by the corresponding institutional ethical committee at the Center of Molecular Biology "Severo Ochoa" and Autónoma University (CEEA-CBMSO-23/159 and were performed in accordance with Spanish regulations (BOE 67/8509-12, 1988) and European regulations (EU directive 86/609, EU decree 2001-486). Reporting followed the ARRIVE Guidelines. For some experiments Aralar/AGC1/Slc25a12-deficient and SCaMC-3/lc25a23-deficient mice were used, both with a mixed SVJ129-C57BL/6 genetic background (Amigo et al., 2013; Jalil et al., 2005).

2.2 | Astrocytes primary culture

Cultures were obtained from postnatal mouse pups (PND 0–PND 1) from crosses between SVJ129-C57BL/6 mice. Briefly, cerebral cortices were removed free of meninges, cut into small pieces, and enzymatically dissociated in phosphate-buffered saline containing 1% BSA, 0.4 mg/ml papain, and 6 mM glucose and then mechanically dissociated, in the presence of DNase, by using glass pipettes of different pore size. Dissociated cells were collected by centrifugation (800*g*, 5 min). Cultures were maintained for 2 weeks, with DMEM-F12 and 10% FBS media replacement every 3–4 days preceded shaking to remove nonastrocyte cells. In the second week glutamine was removed from the culture medium (Juaristi et al., 2017).

2.3 | Cytosolic Na^+, Ca^{2+}, and pH imaging in primary astrocytes cultures

Astrocytes growing on coverslips were loaded with 5 μM Fura 2-AM (ThermoFisher) and 50 μM pluronic acid F.127 (ThermoFisher) for 1 hr min at 37 °C in a medium containing 2.5 mM glucose (137 mM NaCl, 1.25 mM $MgSO_4$, 10 mM HEPES, 3 mM KCl, 2 mM $NaHCO_3$, 2 mM $CaCl_2$, and 1% BSA, pH 7.4, loading media) and washed in Fura 2-AM free media and replaced by buffer without Fura 2-AM (137 mM NaCl, 1.25 mM $MgSO_4$, 10 mM HEPES, 3 mM KCl, 2 mM $NaHCO_3$, and 2.5 mM glucose, Hepes-buffered media) with 2 mM $CaCl_2$ or 100 μM EGTA (Ca^{2+}-free medium, -Ca^{2+}) and immediately used. In experiments without extracellular Na^+, 137 mM NaCl was replaced substituted by 137 mM choline chloride (modified from Martinez-Serrano, Blanco, & Satrústegui, 1992).

Then coverslips were mounted on the microscope stage equipped with a 40× objective as described previously (Ruiz et al., 1998) and Fura 2-AM fluorescence was imaged ratiometrically using alternate excitation at 340 and 380 nm, and a 510 nm emission filter with a Neofluar 40×/0.75 objective in an Axiovert 75 M microscope (Zeiss). $[Na^+]_I$ imaging was performed as previously described (Rose & Ransom, 1997). Briefly, 20 μM SBFI-AM (sodium-binding benzofuran isophthalate) (ThermoFisher) was loaded during 90 min in the presence of 50 μM pluronic acid F.127 in Fura 2-AM loading media. Then

washed and immediately used in Hepes-buffered experimental media. Gramicidin (30 μg/ml) and ouabain (0.1 mM) were added at the end of the experiments. Image acquisition was performed with the Aquacosmos 2.5 software (Hamamatsu) and data analysis was done with Origin software (Origin-Lab).

2 μM BCECF-AM (2′,7′-Bis-(2-Carboxyethyl)-5-(and-6)-Carboxyfluorescein, Acetoxymethyl Ester) (Invitrogen), pH probe was load at room temperature (RT) for 10 min in Hepes-buffered media and washed in BCECF free media. Experiments were performed as for Fura 2-AM and SBFI.

Drugs used for those experiments were: 6-cyano-7-nitroquinoxaline-2,3-dione (CNQX), (5S,10R)-(+)-5-Methyl-10,11-dihydro-5H-dibenzo[a,d] cyclohepten-5,10-imine hydrogen maleate (MK-801), (S)-3,5-Dihydroxyphenylglycine (DHPG) (Tocris Bioscience).

2.4 | Determinations of oxygen consumption

Oxygen consumption in intact astrocytes cultures was studied by using a Seahorse XF24 Extracellular Flux Analyzer (Seahorse Bioscience; Llorente-Folch et al., 2013). Cortical primary astrocytes were plated in XF24 V7 cell culture at 8×10^4 cells/well and cultured for 2 weeks at 37 °C, 5% CO_2, in DMEM F12 10% FBS. Cells were equilibrated with bicarbonate-free low-buffered DMEM medium (without pyruvate, lactate, glucose, glutamine or Ca^{2+}) supplemented with 2.5 mM glucose and 2 mM $CaCl_2$ (+Ca^{2+}) or 100 μM EGTA (-Ca^{2+}), in conditions of ± Ca^{2+}, for 1 hr previous to extracellular flux assay. For the experiments without Na^+, cells were equilibrated in (137 mM NaCl, 1.25 mM $MgSO_4$, 10 mM HEPES, 3 mM KCl, 2 mM $NaHCO_3$, Hepes-buffered media) and 10 min before measuring respiration, cells were washed and media was replaced with fresh media with the same buffer or with a buffer without Na^+ (Martinez-Serrano et al., 1992) with 2.5 mM glucose and 2 mM Ca^{2+}. For OCR experiments studying the implication of KCl, cells were equilibrated in Hepes-buffered experimental media containing 2.5 mM glucose and 2 mM Ca^{2+}. Substrates/ligands were prepared in the same medium in which the experiment was conducted and were injected from the reagent ports automatically at the times indicated. Mitochondrial function in astrocytes was determined through sequential addition of 6 μM oligomycin, 0.5 mM 2,4-dinitrophenol, and 1 μM antimycin/1 μM rotenone. This allowed determination of basal oxygen consumption, oxygen consumption linked to ATP synthesis (ATP linked), non-ATP linked oxygen consumption (proton leak), maximal uncoupled respiration (MUR), and nonmitochondrial oxygen consumption (Brand & Nicholls, 2011). Quantification of these values where done by normalizing from basal-values and after correction for nonmitochondrial OCR. Protein was extracted from wells with 0.1% NP-40-PBS solution, and quantified with BCA protein assay (ThermoFisher).

2.5 | Measurements of mitochondrial Ca^{2+}, cytosolic pyruvate concentration, and ATP/ADP ratio using fluorescent protein sensors

To image mitochondrial Ca^{2+} levels, cytosolic pyruvate and ATP/ADP ratio cells were plated onto 4-well Lab-Tek chamber slides and transfected using calcium-phosphate method 48 hr prior the experiments either with the plasmid encoding, respectively, for the mitochondrial targeted ratiometric 4mtD3cpv (Addgene plasmid 58,184), the cytosolic pyruvate probe pyronic, (kindly provided by F. Barros; San Martin et al., 2014) or the ATP/ADP ratio cytosolic sensor PercevalHR (Addgene plasmid 49,082; Tantama et al., 2013). Experiments were performed in 2.5 mM glucose Hepes-buffered experimental media with either 2 mM $CaCl_2$ (+Ca^{2+}) or 100 μM EGTA (–Ca^{2+}). Additions were made as a bolus. Cells were excited for 300 or 200 ms (4mtD3cpv or pyronic, respectively) at 436/20 nm and the emitted fluorescence was collected through a dual pass dichroic CFP-YFP (440–500 and 510–600 nm). Images were collected every 5 s using a filter wheel (Lambda 10-2, Sutter Instruments; all filters purchased from Chroma) and recorded by a Hamamatsu C9100-02 camera mounted on an Axiovert 200 M inverted microscope equipped with a 40×/1.3 Plan-Neofluar objective. 4mtD3cpv emission ratio was CFP/YFP reflecting mitochondrial Ca^{2+} and for pyronic emission ratio was mTFM/venus reflecting pyruvate concentration. For ATP/ADP ratio measured with PercevalHR, cells were excited alternatively excited for 200 ms at 426–44 (Venus) and 472–27 (GFP) for PercevalHR measurements. The emitted fluorescence was collected at 520/35 (GFP). Images were collected every 5 s using a filter wheel (Lambda 10-2, Sutter Instruments, all filters purchased from Chroma). PercevalHR emission ratio was GFP/CFP reflecting ATP/ADP ratio. ROIs were selected on single-cell fluorescence recordings and analyzed using MetaMorph (Universal Imaging) and ImageJ (NIH). For pyruvate production quantification, the lineal increase in pyronic mTFP/venus fluorescence ratio during the first 30 s after stimulation was determined.

3 | RESULTS

3.1 | ATP-induced Ca^{2+} transients increase astrocyte respiration

Astrocytes are glycolytic cells (Bittner et al., 2011; Dienel & Cruz, 2016; Lopez-Fabuel et al., 2016; Magistretti & Allaman, 2018; Supplie et al., 2017), in which increases in ATP demand produced by different workloads are met by increased glycolysis but may also be met by OXPHOS (Dienel, 2013; Hertz et al., 2007). We have first studied the astrocyte response to agonists whose main actions are intracellular Ca^{2+} mobilization, particularly extracellular ATP. ATP binds purinergic metabotropic receptors (P2Y), causing an increase in cytosolic Ca^{2+} through the release of Ca^{2+} from internal stores via IP3R2 (Franke, Verkhratsky, Burnstock, & Illes, 2012). Emptying endoplasmic reticulum (ER) calcium stores activates calcium entry through low conductance plasmalemmal channels regulated by the level of calcium stored in the ER, inducing a process named store-operated calcium entry (SOCE) (González-Sánchez, Pla-Martín, et al., 2017; Putney, 2009). P2Y-induced Ca^{2+} signals are induced by 100 μM ATP (Kirischuk, Moller, Voitenko, Kettenmann, & Verkhratsky, 1995) and are instrumental for producing propagating intercellular Ca^{2+} waves (Parpura et al., 2017). Astrocytes also express ionotropic receptors (P2X) (Franke et al., 2012) allowing Ca^{2+} entry into the cell and these receptors are related to pathogenic actions of ATP (Grygorowicz, Wełniak-Kamińska, & Strużyńska, 2016).

Figure 1a, shows that addition of 100 μM ATP, which activates P2Y receptors to astrocytes incubated with 2.5 mM glucose, a physiological glucose concentration (Silver & Erecińska, 1994), produces a large and sustained increase of $[Ca^{2+}]_I$, which gradually returns to resting $[Ca^{2+}]_I$. The absence of external Ca^{2+} diminishes the ATP-induced $[Ca^{2+}]_I$ peak, which rapidly returns to resting $[Ca^{2+}]_I$ levels (Figure 1b). Mitochondrial matrix Ca^{2+} levels in astrocytes analyzed with 4mtD3cpv, a FRET calcium indicator targeted to the mitochondrial matrix, (Figure 1c,d), indicate that cytosolic Ca^{2+} signals readily reach mitochondria both in the presence and absence of external Ca^{2+}, with lower matrix Ca^{2+} signals, $[Ca^{2+}]_{mit}$, in Ca^{2+}-free medium (Figure 1d).

To test the involvement of cytosolic Na^+ in the response to 100 μM ATP, $[Na^+]_I$ variations were measured in the same conditions using SFBI-AM as $[Na^+]_I$ sensor. The results show that the addition of 100 μM ATP results in a very small or undetectable increase of $[Na^+]_I$ both in the presence or absence of Ca^{2+} (Figure 1e,f).

Taken together, the results indicate that 100 μM ATP induces a Ca^{2+}-dependent increase in cell workload, which is higher in the presence than absence of external Ca^{2+}, whereas the Na^+-dependent workload induced is minimal and the same in the absence or presence of external Ca^{2+}. Indeed, 100 μM ATP addition to astrocytes transfected with cytosolic ratiometric PercevalHR (Tantama, Martínez-Francois, Mongeon, & Yellen, 2013) resulted in a transient fall in the GFP/venus emission ratio which reflects cytosolic ATP/ADP ratio which was smaller in the absence than in the presence of Ca^{2+} (Figure 1g). These ATP actions are most likely due to activation of P2Y receptors (Kirischuk et al., 1995; Salter & Hicks, 1994, Verkhratsky, Orkand, & Kettenmann, 1998).

We next analyzed the astrocyte response to these workloads in terms of stimulation of cell respiration. Cultured astrocytes have a basal respiration rate of 4.8 ± 0.5 nmol O_2/min/mg protein as described in Juaristi et al. (2017). The addition of 100 μM ATP produces an acute stimulation of respiration (Figure 1h,i) to 118.1 ± 2.6% initial values, which decreases in the absence of external Ca^{2+} (107.4 ± 3.9%, F = 5.952, p-value = .025, one-way ANOVA). These results clearly show that ATP stimulation of mitochondrial respiration is calcium dependent and requires extracellular calcium entry in addition to calcium release from internal stores to produce mitochondrial activation in cultured astrocytes. However, whether stimulated respiration is dependent on the increased workload alone or on the additional effect of Ca^{2+} in activating mitochondrial function is unknown.

3.2 | 1 mM ATP induces a robust stimulation of astrocyte respiration

Figure 2a shows that 1 mM ATP, which activates ionotropic purinergic receptors of astrocytes (Salas et al., 2013), causes a larger increase in $[Ca^{2+}]_I$ than that produced by 100 μM ATP. The $[Ca^{2+}]_I$ signal decreases in absence of external Ca^{2+} (Figure 2b). Figure 2c,d shows that the increase in $[Ca^{2+}]_{mit}$ obtained with 1 mM ATP is also more robust than with 100 μM ATP, with an average increase in $[Ca^{2+}]_{mit}$ larger in the presence than in the absence of external Ca^{2+}.1 mM ATP causes a small, barely detectable, increase of $[Na^+]_I$ in presence of external Ca^{2+}, but a sustained increase of $[Na^+]_I$ in Ca^{2+} free media (Figure 2e,f). This is probably due to the involvement of P2X7 receptors in the action of 1 mM ATP, as these receptors are permeable to both Ca^{2+} and Na^+ (Franke et al., 2012), the absence of Ca^{2+} favoring Na^+ entry. As Na^+ extrusion represents a much higher workload than Ca^{2+} extrusion (Attwell & Laughlin 2001; Llorente-Folch et al., 2013), the workload induced by 1 mM ATP is higher in a Ca^{2+}-free than in a Ca^{2+}-containing medium. In fact, the drop in the ATP/ADP ratio caused by 1 mM ATP (Figure 2g) is much larger than that caused by 100 μM ATP (Figure 1g) and it fails to recover in the absence of external Ca^{2+}.

The respiratory response to 1 mM ATP was quite larger than to 100 μM ATP (Figure 2h). OCR increased 190.4 ± 18.2% of basal values, and the increase was similar in the presence or absence of external Ca^{2+} (Figure 2i). The lack of differences in OCR stimulation in these two conditions is intriguing, as the workloads involved are quite different. It may suggest that the smaller workload achieved in Ca^{2+} medium cooperates with Ca^{2+}-regulation of respiration to reach a stimulation similar to that of the Na^+-workload in Ca^{2+}-free medium lacking the Ca^{2+}-regulatory boost. Alternatively, it is possible that Ca^{2+} is required to supply substrates to mitochondria (derived from glycogen or free glucose), rather than as a respiration booster.

Surprisingly astrocytes are unable of sustaining MUR after the 1 mM ATP signal in absence of Ca^{2+}; MUR was 368.1 ± 35.0% and 87.3 ± 15.1% (F = 74,817, p-value = .000012, one-way ANOVA) in the presence or absence of external Ca^{2+}, respectively (Figure 2h,j). This may be explained by the Ca^{2+}-dependence of a metabolic step required for a maximal supply of respiratory fuels to sustain MUR, especially after a drain of substrates caused by the acute stimulation of respiration in response to 1 mM ATP.

3.3 | Role of mitochondrial Ca^{2+} regulation systems and Ca^{2+} regulation of pyruvate supply in the acute stimulation of astrocyte respiration by ATP

The substantial stimulation of astrocyte respiration by 1 mM ATP in the presence of Ca^{2+} may reflect a Ca^{2+} regulatory boost or a Ca^{2+}-stimulated increase in respiratory substrate supply. Ca^{2+} regulation of mitochondrial respiration may involve uptake in mitochondria through MCU and activation of mitochondrial dehydrogenases or directly from the external side of the inner mitochondrial membrane via binding to the ATP-Mg/Pi carrier SCaMC-3 Slc25a23 or the aspartate/glutamate carrier Aralar/AGC1 (Glancy & Balaban, 2012; Llorente-Folch et al., 2013). To study the role of the ATP-Mg/Pi carrier SCaMC-3, the main Ca^{2+}-dependent mitochondrial metabolite transporter in astrocytes (Sharma et al., 2015), we have employed astrocytes derived from SCaMC-3-KO mice (Rueda et al., 2015). SCaMC-3 regulates respiration in neurons in response to high workloads (Llorente-Folch et al., 2013; Rueda et al., 2015). Basal respiration in WT and SCaMC-3-KO astrocytes was the same 5.82 ± 0.35 and 4.98 ± 0.33 pmol O_2/min/μg protein, respectively (F = 2.836, p-value = .10, one-way ANOVA), and stimulation of respiration with 100 μM or 1 mM ATP or MUR in the presence of external calcium was also the same in WT and SCaMC-3 KO astrocytes (Figure 3a,b). Having ruled out a role of SCaMC-3 on the calcium regulatory boost, we studied the possible role of Aralar-MAS. Figure 3c,d shows that the lack of Aralar does not affect basal respiration or ATP-stimulated

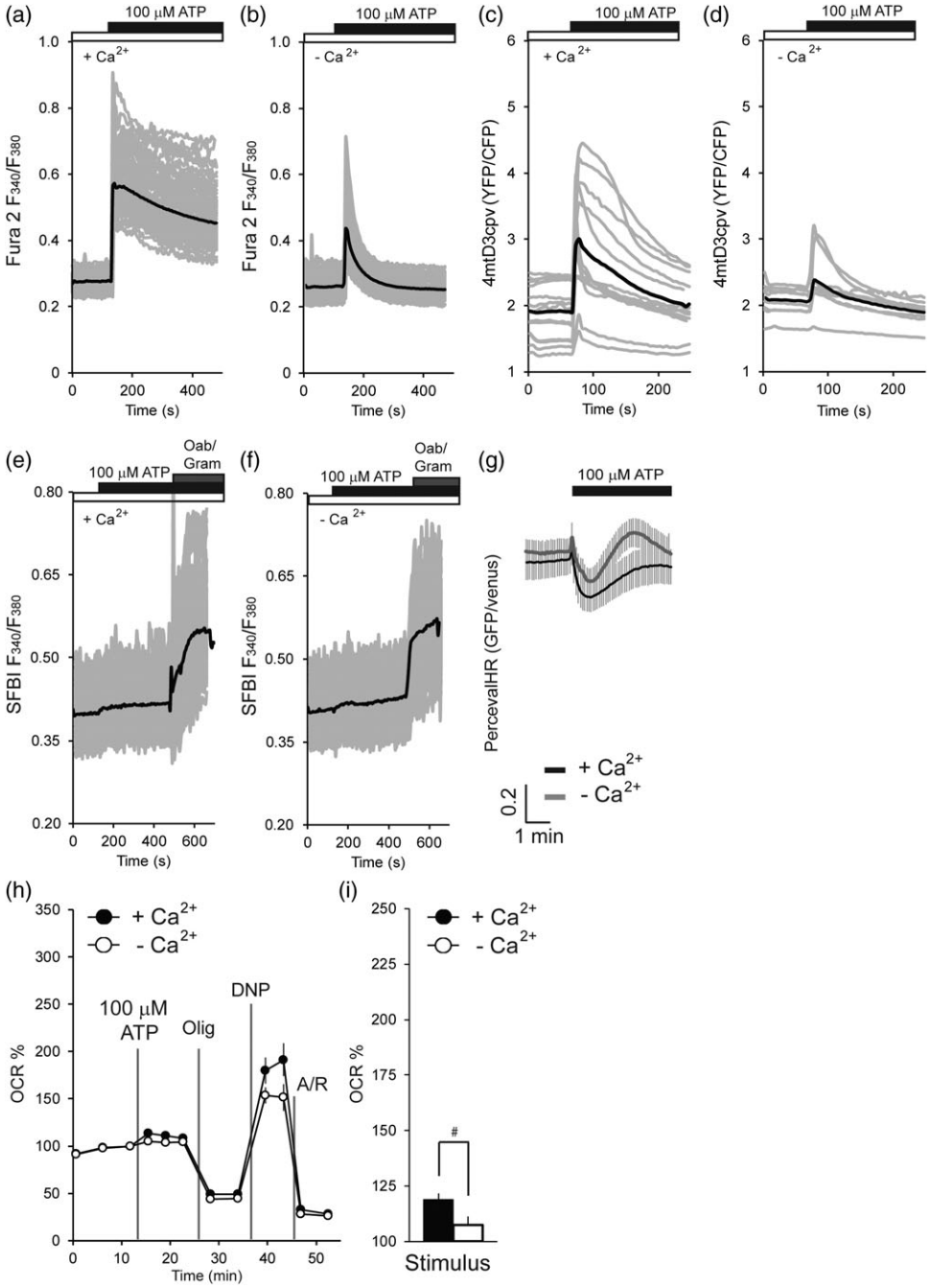

FIGURE 1 Effect of 100 μM ATP on $[Ca^{2+}]_I$, $[Ca^{2+}]_{mit}$, $[Na^+]_I$, cytosolic ATP/ADP ratio and mitochondrial respiration in astrocytes. (a,b) Changes in $[Ca^{2+}]_I$, in Fura 2 loaded astrocytes obtained by stimulation with 100 μM ATP in a calcium containing (a) or Ca^{2+}-free medium (b). Data obtained from 60 to 80 cells of three independent experiments. (c,d) $[Ca^{2+}]_{mit}$ in astrocytes expressing mitochondrial Ca^{2+} sensor 4mtD3cpv, obtained by stimulation with 100 μM ATP in a calcium containing or Ca^{2+}-free medium. Data obtained from 9 to 13 cells of three independent experiments. (e,f) Changes in $[Na^+]_I$, in SFBI loaded astrocytes stimulated with 100 μM ATP in 2 mM Ca^{2+} medium or Ca^{2+}-free medium Ouabain (0.1 mM) and gramicidin (30 μg/ml) were added where indicated as control for a robust response. Data are from three independent experiments repeated twice and 20–30 cells analyzed per experiment. Means are in black and individual cell traces in gray. (g) ATP/ADP ratio after 100 μM ATP addition, in astrocytes expressing PercevalHR, in presence of 2 mM Ca^{2+} (black) or in a Ca^{2+}-free media (gray). Results are means ± *SEM* from three independent experiments, 14–16 cells per conditions. (h) Oxygen consumption profile showing the stimulation of OCR induced by 100 μM ATP added where indicated in the presence or absence of external Ca^{2+}. Results are normalized to initial OCR values, serial injections of ATP (100 μM), oligomycin (Olig, 6 μM), 2,4-dinitrophenol (DNP, 0.5 mM) and antimycin/rotenone (A/R, 1/1 μM) are shown. **(i)** 100 μM ATP induced stimulation of respiration at 3 min after addition, as percentage of basal respiration, which was 4.8 ± 0.5 nmol O_2/min/mg protein (Juaristi et al., 2017). Data are mean ± *SEM* of 9–11 wells from three independent experiments. Means were compared using one-way ANOVA (# $p < .05$)

respiration, or MUR. These results indicated that even under Ca^{2+}-stimulation conditions, Aralar-MAS is not involved in the control of astrocyte respiration as it is in neurons.

These results point to the MCU and its effects on matrix Ca^{2+} and matrix dehydrogenases as the most likely mechanism whereby calcium ions boost respiration in astrocytes. Indeed, both ATP-induced Ca^{2+}

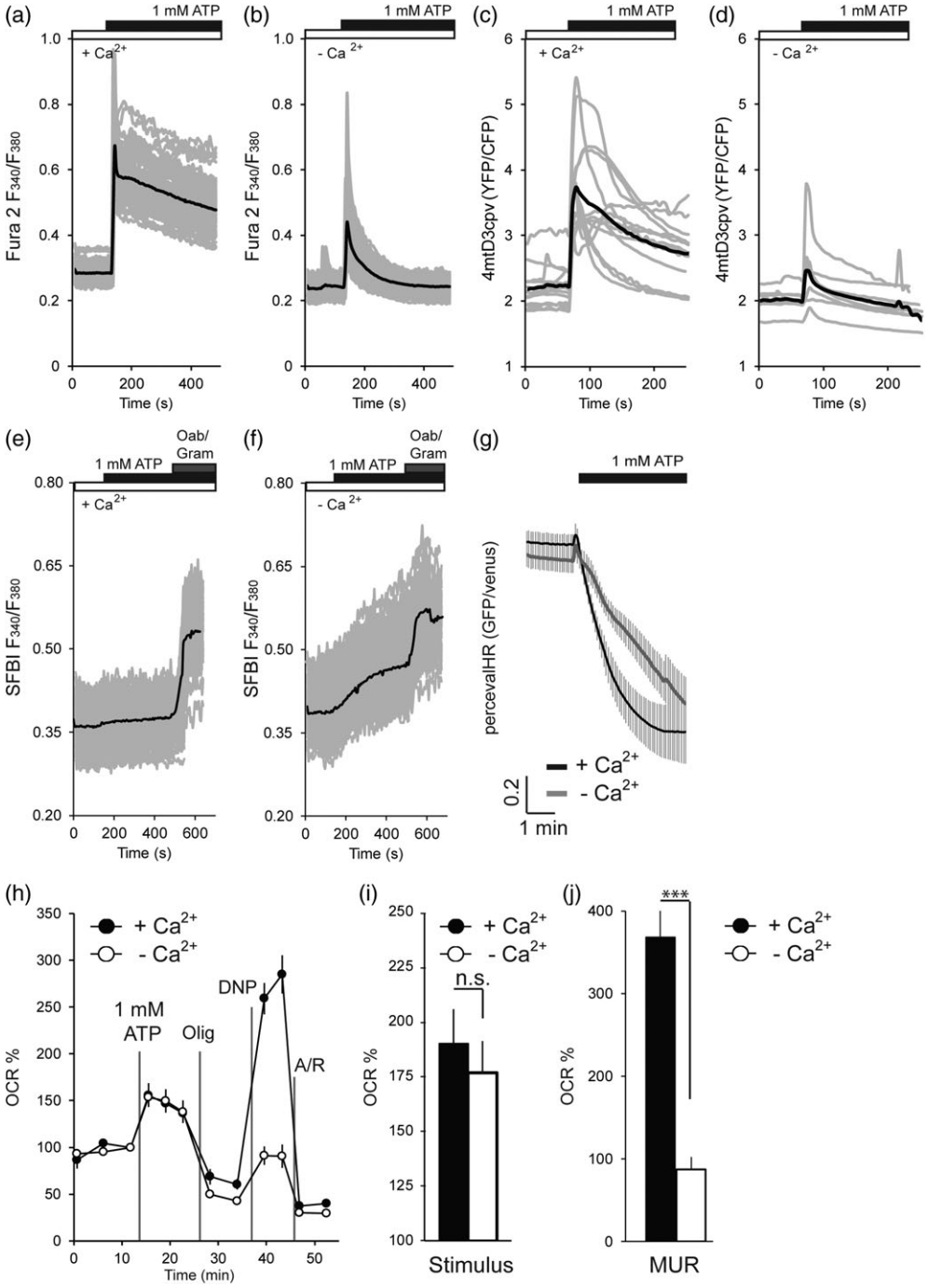

FIGURE 2 Effect of 1 mM ATP on $[Ca^{2+}]_I$, $[Ca^{2+}]_{mit}$, $[Na^+]_I$, cytosolic ATP/ADP ratio, and mitochondrial respiration in astrocytes in the presence or absence of external calcium. (a–i) $[Ca^{2+}]_I$, $[Ca^{2+}]_{mit}$, and $[Na^+]_I$, ATP/ADP ratio and OCR responses to 1 mM ATP, as described in the legend to Figure 1. (j) Maximal uncoupled rate (MUR) obtained 3 min after 0.5 mM 2,4-dinitrophenol (DNP) addition. Results are mean ± *SEM* of 5 wells from three independent experiments. Data were compared using one-way ANOVA (***p-value < .001)

signals readily reach mitochondria (Figures 1c,d and 2c,d). However, we have been unable to verify this possibility experimentally, as our attempts to silence or inhibit the MCU in intact astrocytes have been unsuccessful.

We next tested the possibility that calcium stimulates substrate supply, particularly pyruvate. To this end, astrocytes were transfected with the FRET sensor pyronic (San Martin et al., 2014) and the responses to ATP were analyzed 48 hr later. In the presence of glucose, astrocytes have resting cytosolic pyruvate levels below the detection limit of pyronic (10 μM) as found previously (Ruminot, Schmälzle, Leyton, Barros, & Deitmer, 2017, San Martin et al., 2014, 2017). However, upon the addition of 100 μM or 1 mM ATP, there was a clear rise in the pyronic mTFP/Venus ratio at 1 mM ATP which was much smaller in Ca^{2+}-free media (Figure 3e-h). Quantification of the initial rates of increase showed that pyruvate production was Ca^{2+}-dependent and only detectable at 1 mM (Figure 3i). As the workload and drop in ATP/ADP ratio induced by 1 mM ATP are larger in the absence than presence of external Ca^{2+}, failure to increase pyruvate production in Ca^{2+}-free medium clearly suggests a Ca^{2+} dependent step in the activation of glycolysis and/or glycogenolysis.

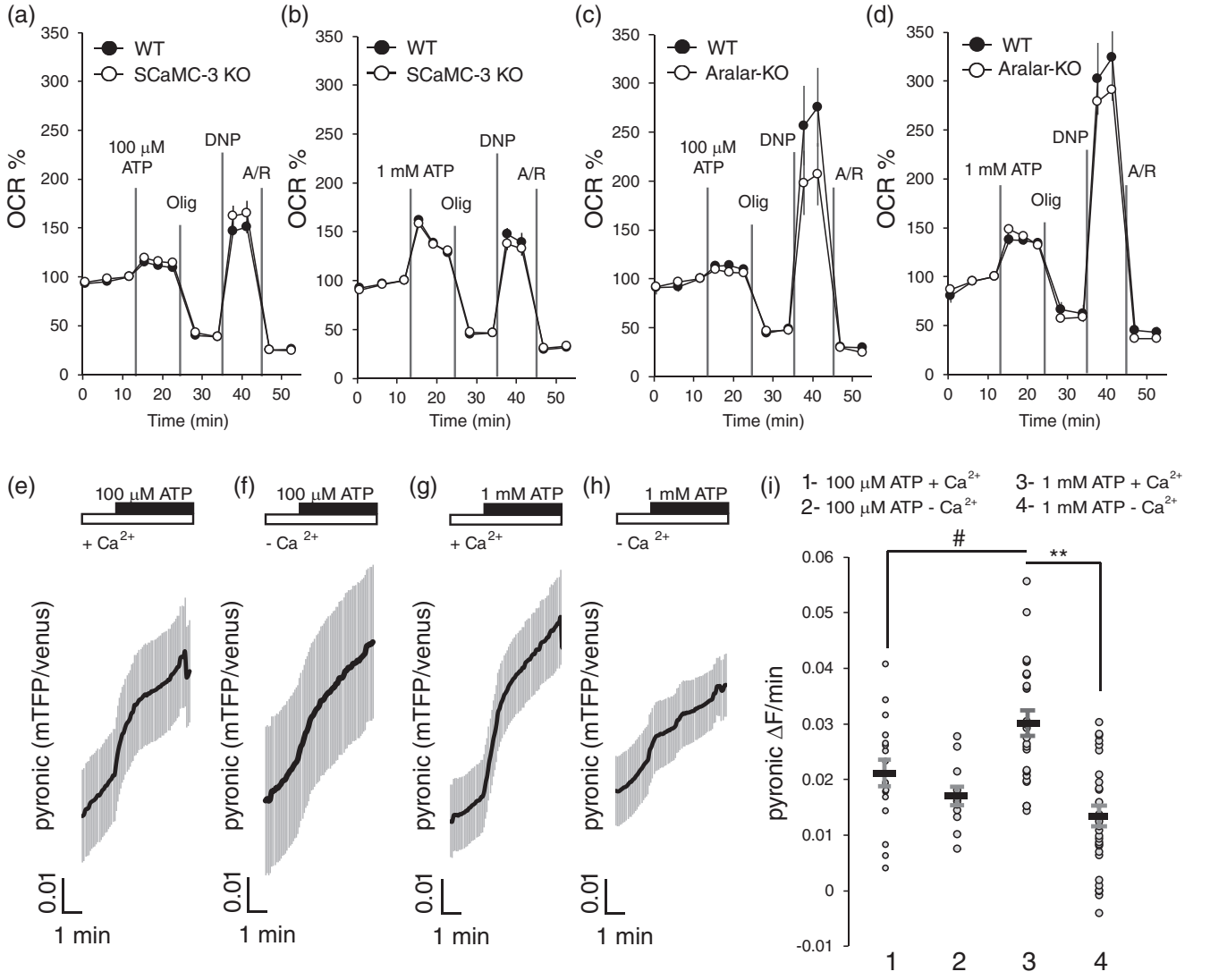

FIGURE 3 OCR response to extracellular ATP in wild type and SCaMC-3-KO ARALAR-KO mouse astrocytes and effect in pyruvate production in wild type astrocytes. (a–d) OCR profile in response to 100 μM and 1 mM ATP in WT and SCaMC-3 KO astrocytes, or WT and Aralar-KO astrocytes. Other additions are as described in legend to Figure 1. Results are means ± *SEM* of 5–8 replicates from two to three independent experiments. (e–h) Increase in cytosolic pyruvate induced by addition of 100 μM (e,f) or 1 mM ATP (g,h), in the presence of Ca^{2+} or in Ca^{2+}-free media to astrocytes transiently transfected with pyronic 48 hr earlier. Data are means ± *SEM* from 12–25 cells of three independent experiments. **(i)** Pyruvate production was quantified from the increase of pyronic fluorescence ratio over the initial 30 s after ATP addition (pyronic Δ*F*/min). Individual data (dots) and mean ± *SEM* of each group are shown, where means are colored horizontal lines. Means were compared using one-way ANOVA followed by Bonferroni post hoc tests (# $p < .05$, ** $p < .01$)

3.4 | Glutamate increases respiration in cultured astrocytes

Glutamate has various actions in astrocytes. It may be taken up, through the main astroglial glutamate transporters GLT-1/EAAT2/Slc1a2 and GLAST/EAAT1/Slc1a3 (Canul-Tec et al., 2017, Kanai et al., 2013), and/or it may activate glutamate receptors in astrocytes, mainly metabotropic receptors (Panatier & Robitaille; 2016; Sun et al., 2013), or even NMDA receptors (Jimenez-Blasco, Santofimia-Castaño, Gonzalez, Almeida, & Bolaños, 2015). Each of these actions is accompanied by increases in cytosolic Ca^{2+} which arise from different mechanisms. These processes entail specific increases in the cell workload, which may trigger a response in terms of energy production via OXPHOS. Our interest focused on the involvement of OXPHOS in response to glutamate, the nature of the workload imposed by glutamate and the role of Ca^{2+} as regulatory mechanism to increase cell respiration.

The glutamate transporters GLT-1/EAAT2/Slc1a2 and GLAST/EAAT1/Slc1a3 take up one glutamate, three Na^+ and one H^+ in exchange of one K^+, the overall process being electrogenic (Jackson & Robinson, 2018; Kanai et al., 2013; Kirischuk, Parpura, & Verkhratsky, 2012). The extrusion of Na^+ requires Na^+-K^+ ATPase activity at the expense of one ATP per three Na^+. Therefore, three Na^+ need to be extruded and one ATP broken down per glutamate molecule introduced into the cell (Kirischuk et al., 2012). The H^+ will be extruded by Na^+/H^+ exchange, or through the sodium bicarbonate cotransporter NBCe1 (Theparambil, Ruminot, Schneider, Shull, & Deitmer, 2014) thus requiring the removal of an extra Na^+ (Attwell & Laughlin, 2001). In addition, the increase in $[Na^+]_I$ can cause cytosolic Ca^{2+} signals due

to Ca^{2+} entry in exchange with $[Na^+]_I$ through reverse NCX (Jackson, O'Donnell, Takano, Coulter, & Robinson, 2014; Kirischuk et al., 2012; Rojas et al., 2007). However, these $[Ca^{2+}]_I$ signals may also arise from the action of glutamate on metabotropic receptors (Sun et al., 2013). Inside the astrocyte, glutamate can be either transformed into glutamine in the cytosol or into α-ketoglutarate in mitochondria and further transformed or consumed.

Figure 4 shows the changes in Na^+ and Ca^{2+} levels caused by 200 μM glutamate addition to astrocytes in the presence or absence of extracellular calcium. Glutamate induced an increase in $[Na^+]_I$ (Figure 4a,b) independent of external $[Ca^{2+}]$ (increase in SFBI fluorescence ratio of 0.066 ± 0.010 and 0.061 ± 0.006, after 2 min of glutamate addition, F = 0.20, p-value = .66, one-way ANOVA), with 2 mM Ca^{2+} and Ca^{2+}-free medium, arguing against the importance of reverse NCX as compared with the Na^+ pump in clearing cytosolic Na^+ in astrocytes. The glutamate transporters rather than AMPA or NMDA receptors are largely responsible for the increase in $[Na^+]_I$, as the increase is only marginally affected by the addition of the corresponding blockers (CNQX, 10 μM, MK801, 10 μM, respectively, Figure 4c).

Glutamate produces a small, sustained and variable increase in $[Ca^{2+}]_I$, (Figure 4d,e). The average increase in Fura 2 fluorescence ratio 2 min after glutamate addition is smaller in Ca^{2+}-free media (Figure 4f). The addition of glutamate (200 μM) resulted in an increase in mitochondrial Ca^{2+} (Figure 4g,h) which was much smaller than those detected following ATP addition (Figures 1c,d and 2c,d). This increase was also smaller in Ca^{2+}-free than in Ca^{2+}-containing media.

Glutamate (200 μM) induced a sustained increase in respiration in astrocytes both in the presence and absence of Ca^{2+} (Figure 4i,j). This result contrasts with previous reports (Azarias et al., 2011) in which glutamate addition inhibited respiration in astrocytes incubated with deoxyglucose (DG) which might have caused a rundown of ATP. However, in a more recent study carried out in the absence of DG this same group reported that glutamate increased astrocyte OCR (Rimmele et al., 2018). In the present study the normalized increase in respiration (from initial values to 3 min after glutamate addition) was similar in presence and in absence of $[Ca^{2+}]_o$ (153.8 ± 5.5% and 152.1 ± 7.1%, respectively). Coupled respiration and proton leak are also similar under the in two $[Ca^{2+}]_o$ conditions (Figure 4j). These results suggest that the OCR response to glutamate follows the ATP demand imposed by the Na^+ workloads which were similar in the two conditions (Figure 4a,b). Indeed, the workload induced by Na^+ entry exceeds by far that induced by Ca^{2+} entry (Llorente-Folch et al., 2013). They also suggest that Ca^{2+} regulation of respiration does not play a relevant role in the OCR response to glutamate.

3.5 | Glutamate acting through metabotropic receptors does not increase respiration in cultured astrocytes

It may be argued that the dominant role of Na^+ entry in driving glutamate-stimulated respiration prevents detecting a role for Ca^{2+} regulation in the response. To study this possibility, we have analyzed the effects of glutamate activation of metabotropic receptors by using (S)-3,5-dihydroxyphenylglycine (DHPG), a specific agonist of group I receptors (mGluR1 and mGluR5) (González-Sánchez, Del Arco, Esteban, & Satrústegui, 2017). Figure 5a shows that 50 μM DHPG induces a transient and variable increase in $[Ca^{2+}]_I$ which diminished in Ca^{2+}-free medium (results not shown). This increase in $[Ca^{2+}]_I$ reached mitochondria increasing $[Ca^{2+}]_{mit}$ (Figure 5b). DHPG addition did not change $[Na^+]_I$, either in presence (Figure 5c) or absence (not shown) of 2 mM Ca^{2+}. Therefore, the metabotropic receptor mediated response to glutamate is exclusively Ca^{2+}-mediated, with no changes in intracellular Na^+. Strikingly, 50 μM DHPG elicited no response in terms of cellular respiration rate (Figure 5d), indicating that glutamate activation of metabotropic receptors and its associated Ca^{2+} signals do not contribute to glutamate-stimulation of respiration.

3.6 | Glutamate-stimulated respiration in astrocytes meets energy demands of increased $[Na^+]_I$

To further substantiate the role of $[Na^+]_I$ in glutamate-stimulation of respiration, we have studied the response to glutamate in the presence or absence of external Na^+. To this end, choline was used to isosmotically replace Na^+, so that astrocyte media contained 137 mM Na^+ ($+Na^+$) or 2 mM Na^+ ($-Na^+$). As predicted, the addition of glutamate induced a very much smaller increase in $[Na^+]_I$ in low than in $+Na^+$ medium (Figure 6a). The lack of external Na^+ resulted in an increase in basal $[Ca^{2+}]_I$ (Figure 6b) and a decrease in basal $[Na^+]_i$ (Figure 6a), consistent with the block of forward NCX, a major mechanisms regulating $[Ca^{2+}]_I$. The addition of glutamate in low Na^+ medium caused a similar $[Ca^{2+}]_I$ rise than in + Na^+ medium (Figure 6b). The lack of Na^+ resulted in a drastic drop in glutamate-stimulation of respiration (Figure 6c,d). These results indicate that mitochondrial respiration in astrocytes responds to Na^+-related ATP-demand.

3.7 | The increase in respiration induced by glutamate is also produced by D-aspartate which is not metabolized by astrocytes

It may be argued that the effects of glutamate on respiration are related to its role as respiratory substrate. Indeed, glutamate can be consumed by astrocytes after transformation to α-ketoglutarate entering in the TCA (Nissen, Pajecka, Stridh, Skytt, & Waagepetersen, 2015). To study this possibility we have used D-aspartate which is taken up through glutamate transporters but cannot be metabolized by astrocytes (Bittner et al., 2011). 500 μM D-aspartate and 200 μM glutamate evoked a similar increase in $[Na^+]_I$ (Figure 6a,f). 500 μM D-aspartate produced a small increase in $[Ca^{2+}]_I$ (Figure 6e), smaller than that caused by 200 μM glutamate (Figure 6b), as metabotropic glutamate receptors will not be recruited by D-aspartate. Figure 6g shows that D-aspartate (500 μM) also induced a sustained increase in respiration, independent of $[Ca^{2+}]_O$ (137.5 ± 6.8% or 127.1 ± 9.6% from basal values, in the presence or absence of external calcium, respectively) and close to that caused by glutamate (Figure 6c,d). However, it should be noted that the stimulation of respiration by glutamate was consistently larger than that obtained with D-aspartate, even though it was used at a lower concentration. This cannot be attributed to different Km for the two ligands which are very similar (Gegelashvili & Schousboe, 1998).

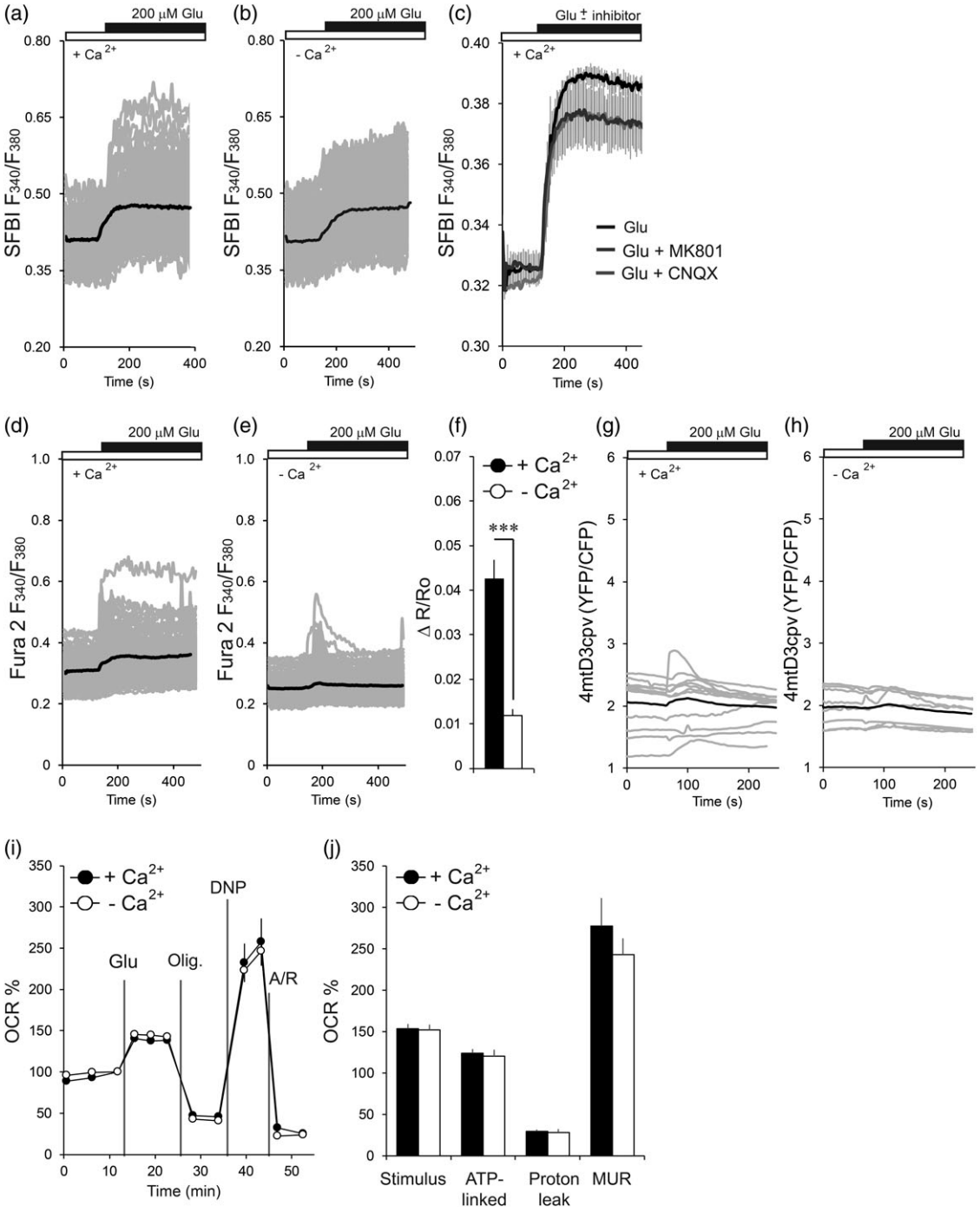

FIGURE 4 Effect of 200 μM glutamate on $[Na^+]_I$, $[Ca^{2+}]_i$, $[Ca^{2+}]_{mit}$, and mitochondrial respiration in astrocytes in the presence or absence of external calcium. (a,b) Changes in $[Na^+]_I$, in SFBI loaded astrocytes stimulated with 200 μM glutamate (Glu) in 2 mM Ca^{2+} or Ca^{2+}-free media. Data obtained from three independent experiments; 20–30 cells were analyzed per experiment. Individual cell recordings are gray lines and means are black traces. (c) Changes in $[Na^+]_I$ in SFBI loaded astrocytes stimulated with glutamate (200 μM) in the absence or presence of AMPA (10 μM CNQX) or NMDA (10 μM MK801) inhibitors. Data are means ± *SEM* obtained from two to three experiments and 20–30 cells per experiment. (d,e) Changes in $[Ca^{2+}]_I$, in Fura 2 loaded astrocytes obtained by stimulation with 200 μM Glu in 2 mM Ca^{2+} and Ca^{2+}-free medium. Data obtained from four independent experiments, 20–30 cells per experiment. (f) Quantification of the increase of Fura 2 ratio signal obtained 2 min after Glu addition ($\Delta R/R_0$). Data are mean ± *SEM* of experiments showed in (d,e). (g,h) $[Ca^{2+}]_{mit}$ signals after transient transfection with 4mtD3cpv sensor, Ca^{2+} conditions are indicated (n = 7–11 cells from two independent experiments). (i) OCR profile in response to 200 μM Glu under the indicated Ca^{2+} conditions. Other additions as indicated in Figure 1. (j) OCR normalized values with respect to basal respiration after correction for nonmitochondrial OCR. Stimulus: 200 μM Glu induced stimulation of respiration at 3 min after addition. ATP-linked values: Oligomycin-sensitive-OCR. Proton-leak: OCR remaining after oligomycin addition. Maximal uncoupled respiration (MUR): OCR values obtained 3 min after the addition of DNP. Data are means ± *SEM* of 6–7 wells from three independent experiments. Means were compared using one-way ANOVA, (*** $p < .001$)

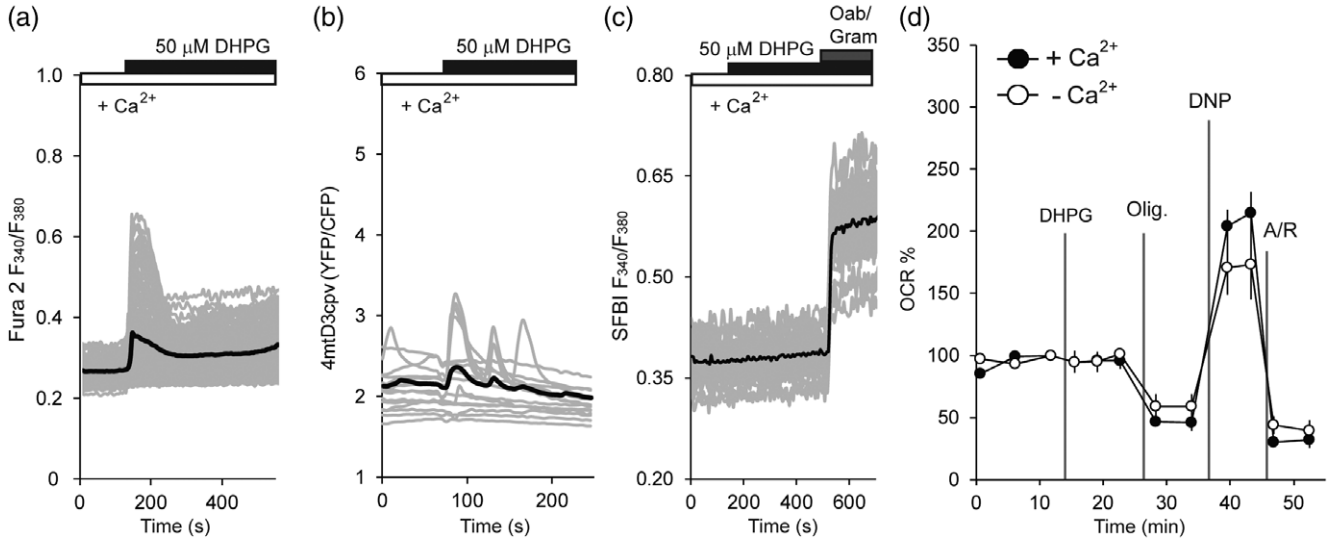

FIGURE 5 Activation of metabotropic glutamate receptor with DHPG (50 μM) does not stimulate mitochondrial respiration. (a) Changes in $[Ca^{2+}]_I$, in Fura 2 loaded astrocytes obtained by stimulation with 50 μM DHPG (3,5-Dihydroxyphenylglycine) in the presence of 2 mM Ca^{2+}. Data obtained from three independent experiments with 20–30 cells per experiment. (b) $[Ca^{2+}]_{mit}$ in astrocytes expressing 4mtD3cpv after 48 hr after transfection as in conditions described in a. Data obtained of 15 cells from three independent experiments. (c) Changes in $[Na^+]i$ in SFBI loaded astrocytes in presence of Ca^{2+} 2 mM. Ouabain and gramicidin (Oab/gram, 0.1 mM/30 μg/ml) were added where indicated. Individual cell recordings are shown as in gray lines and the means as black traces. (d) 50 μM DHPG induced OCR profile in 2 mM Ca^{2+} or Ca^{2+}-free media, serial injections of DHPG (50 μM), other additions as indicated in Figure 1. Data are means ± *SEM* of 5 wells from two independent experiments

3.8 | Glutamate-induced upregulation of glycolytic pyruvate production stimulates astrocytic respiration

Na^+ extrusion in astrocytes represents a large workload coupled to ATP supply by glycolysis and through OXPHOS (Fernández-Moncada & Barros, 2014). Glutamate stimulates astrocytic glycolysis (Pellerin & Magistretti, 1994; Bittner et al., 2011) and we wondered whether OXPHOS stimulation by glutamate was preceded or followed by changes in cytosolic pyruvate levels. Figure 7a,b shows that the addition of glutamate or D-aspartate in astrocytes expressing pyronic results in a rapid increase in cytosolic pyruvate. The increase in pyruvate caused by glutamate and D-aspartate arises from glycolysis, as it is substantially blocked by 30–45 min incubation in the presence of the glycolytic inhibitor iodoacetate (IAA) (Figure 7c,d). These results suggest that the rapid increase in OCR caused by glutamate is associated with the increase in cytosolic pyruvate which follows the stimulation of glycolysis. However, the inhibition exerted by IAA is almost complete (80%) for D-aspartate-stimulated pyruvate formation, but clearly lower (50%) for glutamate stimulated pyruvate formation. These results indicate that in addition to stimulating glycolytic pyruvate formation, glutamate itself is a source of pyruvate, as reported earlier (Hertz et al., 2007). Together with the larger increase in respiration by glutamate than by D-asp, these results show that glutamate increases respiration and pyruvate formation both through a Na^+-dependent workload and by providing a respiratory substrate.

As recently shown by Fernández-Moncada et al. (2018), glutamate addition results in a decrease in ATP levels measured with ATeam 1.03. To further substantiate this change, the ATP/ADP ratio was also studied by employing cytosolic targeted ratiometric PercevalHR as sensor and a decrease in the ATP/ADP ratio was also observed upon glutamate or D-aspartate addition (Figure 7e). As Perceval is pH sensitive (Tantama et al. 2013), we verified that this was not merely due to the acidification of the cytosol which accompanies glutamate transport (Figure 7e), as 0.1 mM HCl which causes a similar acidification (Figure 7f) caused much smaller changes in PercevalHR (Figure 7e). Therefore, the results indicate that glutamate or D-aspartate-induced workload causes a decrease in the ATP/ADP ratio which stimulates glycolysis and pyruvate production.

3.9 | Glutamate-induced upregulation of respiration occurs in the presence of elevated extracellular K+

An elevation of extracellular K^+ as that occurring during neuronal excitation has been shown to result in no changes (Rimmele et al., 2018) or an inhibition of respiration in astrocytes (Fernández-Moncada et al., 2018). Figure 8a shows that the addition of 12 mM KCl results in an inhibition of respiration of about 15% (Figure 8b). This was not due to a hyperosmotic effect as the addition of 24 mM sucrose did not change basal respiration (Figure 8a). The inhibition of OCR by KCl was smaller than that reported by Fernández-Moncada et al. (2018) but the effect was larger than that found by Rimmele et al. (2018). This may be due to differences in bicarbonate content of the media used by the different groups. As both glutamate and K^+ increase in the extracellular space during neuronal activity, we wondered whether glutamate or D-aspartate uptake in astrocytes was able to overcome the effect of K^+. Figure 8c,d shows that OCR stimulation by glutamate or D-aspartate is maintained in the presence of high K^+.

4 | DISCUSSION

As pointed out by different groups, astrocytes are mainly glycolytic but have also the capacity to meet energy demands through ATP production by OXPHOS (Dienel, 2013, Dienel & McKenna, 2014, Hertz

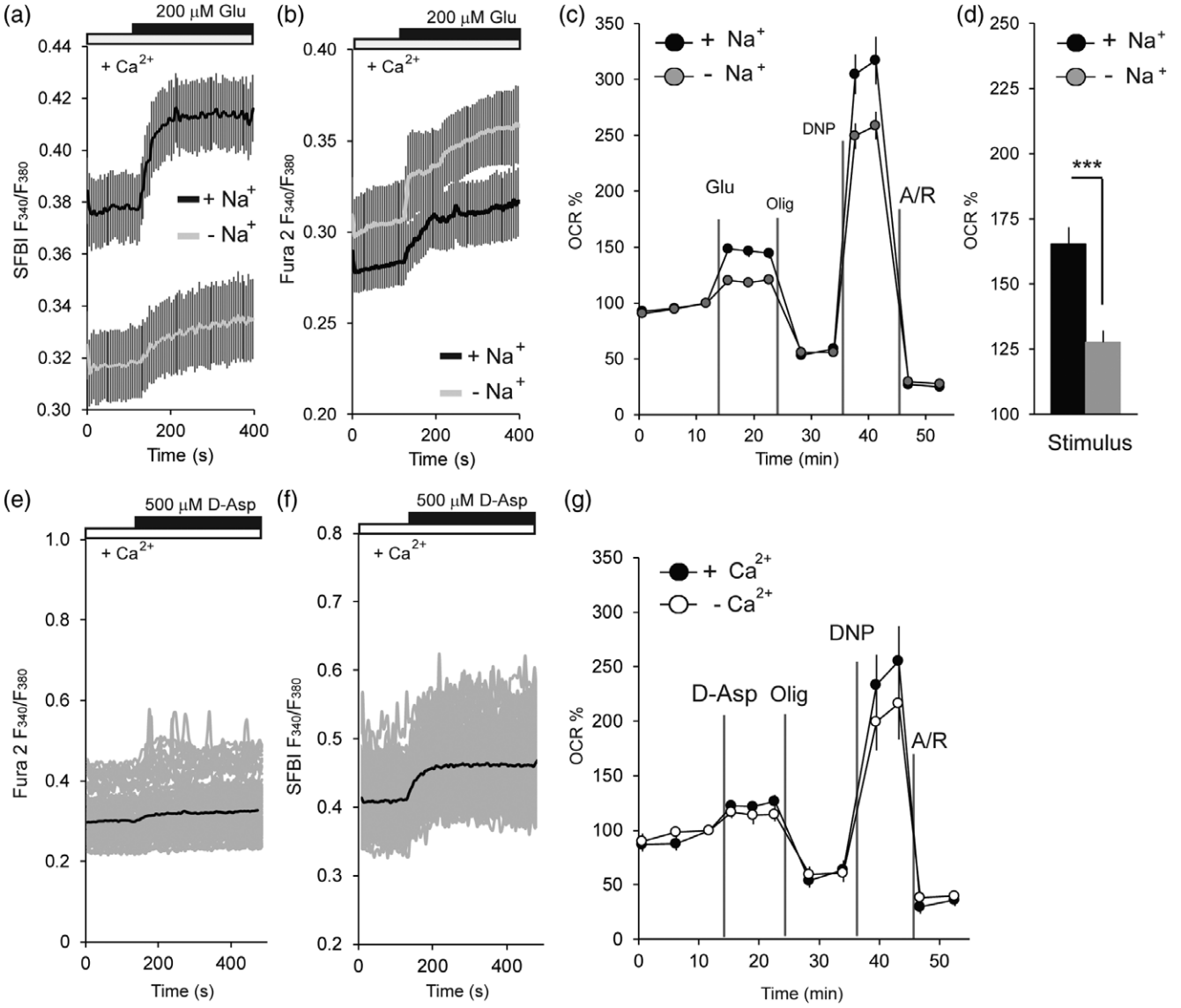

FIGURE 6 Effect of 200 μM glutamate on $[Na^+]_I$, $[Ca^{2+}]_I$, and mitochondrial respiration in astrocytes in the presence or absence of external sodium. (a,b) Changes in $[Na^+]_I$ and $[Ca^{2+}]_I$ in astrocytes loaded with SFBI and Fura2 probes, respectively, after 200 μM glutamate addition (Glu). Experiments were performed in isosmotic 137 mM Na^+ ($+Na^+$) or 2 mM Na^+ ($-Na^+$) media. Data are means ± *SEM* from three independent experiments, with 20–30 cells per experiment. (c) 200 μM Glu induced OCR stimulation under the same Na^+ conditions. Results are normalized to initial OCR values and inhibitors are added as in Figure 1. (d) Stimulation of respiration 3 min after 200 μM Glu addition. Data are means ± *SEM* of 10 wells from two independent experiments. (e) Changes in $[Ca^{2+}]_I$ produced by the addition of 500 μM D-aspartate (D-asp) in presence of 2 mM Ca^{2+} in Fura 2 loaded astrocytes. Three independent experiments, 20–30 cells per experiment. (f) Changes in $[Na^+]_I$ produced by 500 μM D-aspartate addition in SFBI loaded astrocytes in presence of 2 mM Ca^{2+}. Three independent experiments, 20–30 cells per experiment. Means correspond to black tracings and gray represent individual cell recordings. (g) D-asp induced OCR profile in 2 mM Ca^{2+} or Ca^{2+}-free media. Serial injections of D-asp (500 μM) and mitochondrial inhibitors as indicated in Figure 1. Data are means ± *SEM* from 6 to 8 wells, from four independent experiments. Means were compared using one-way ANOVA, (*** $p < .001$)

et al., 2007, Hertz & Hertz, 2003, Lovatt et al., 2007, Nissen et al., 2015, Sonnewald, 2014). We have now shown that extracellular ATP, a ubiquitous signaling molecule in the CNS (Franke et al., 2012), which may be released by neurons and astrocytes (Shen, Nikolic, Meunier, Pfrieger, & Audinat, 2017) induces an increase in astrocyte respiration which appears to depend on Ca^{2+}-stimulation of glycolytic pyruvate production and calcium signaling in mitochondria. On the other hand, the astrocyte response to glutamate which is critical to assist neuronal metabolism during neurotransmission, also consists in an upregulation of glycolysis and oxygen consumption through essentially Ca^{2+} independent pathways.

Astrocytes express metabotropic (P2Y) and ionotropic (P2X) purinergic receptors (Matute, 2011) and we used two different extracellular ATP concentrations, 100 μM and 1 mM, respectively, to activate each of them. These ATP concentrations may be reached in the synapse and brain extracellular space, although whether millimolar ATP levels remain for a long period is uncertain. Under physiologic conditions, ectoenzymes present in the brain will rapidly destroy ATP, and terminate its actions on P2X receptors. However, under pathologic situations such as brain ischemia or trauma, extracellular ATP accumulates after release from dying cells, leading to persistent activation of P2X receptors and astrocyte cell death (Franke et al., 2012; Salas

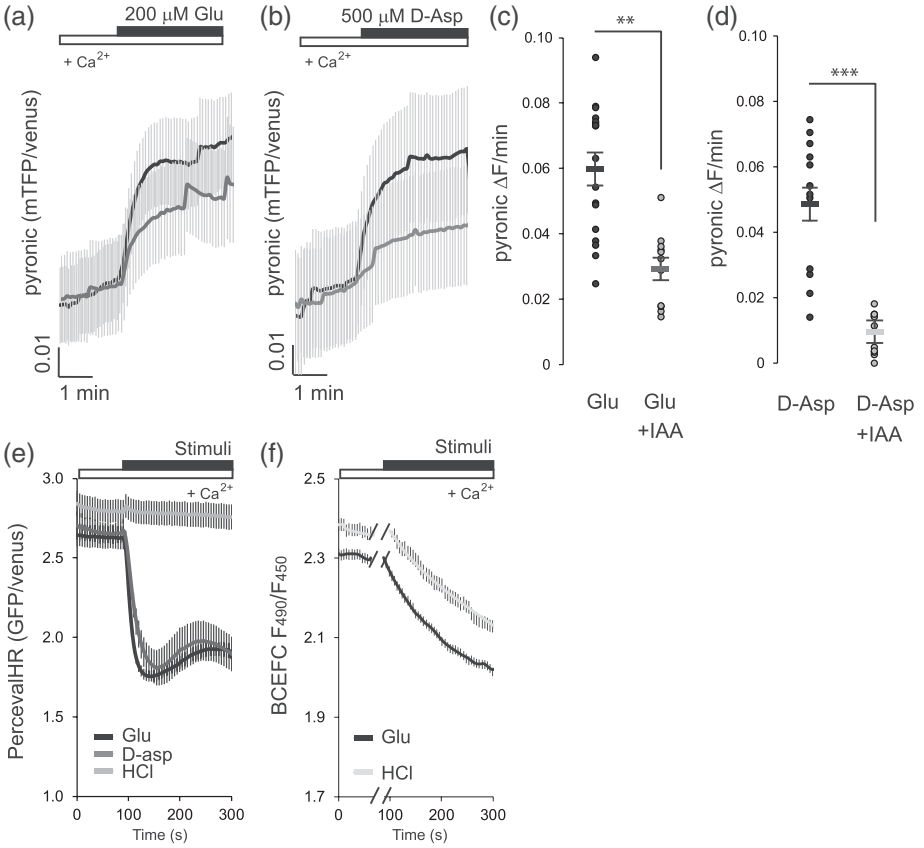

FIGURE 7 Effect of glutamate stimulation on cytosolic pyruvate and cytosolic ATP/ADP ratio. (a,b) Increase in cytosolic pyruvate induced by addition of glutamate (200 μM) (a) or D-asp (500 μM) (b) to astrocytes transiently transfected with pyronic 48 hr earlier. Where indicated, cells were treated with 500 μM iodoacetate (IAA) during 30–45 min before recording pyronic fluorescence. Data are mean ± *SEM* of 11–17 cells from three independent experiments. (c,d) Pyruvate production was quantified from the increase of pyronic fluorescence ratio over the initial 30 s after glutamate (c) or D-asp addition (d) (pyronic Δ*F*/min). Individual data (dots) and mean ± *SEM* of each group are shown, where means are colored horizontal lines. Means were compared using one-way ANOVA, (** $p < .01$, *** $p < .001$). (e) Changes in cytosolic ATP/ADP ratio upon 200 μM glutamate (Glu), 500 μM D-aspartate (D-asp), or 0.1 mM HCl addition in the presence of 2.5 mM glucose and 2 mM Ca^{2+}. Astrocytes were transfected with PercevalHR and used 48 hr later. Data are means ± *SEM* of 8–13 cells from two independent experiments. (f) Variations in intracellular pH in BCECF-loaded astrocytes under the same conditions. Data are means ± *SEM*, with 20–30 cell per experiment

et al., 2013; Verkhratsky, Krishtal, & Burnstock, 2009). This has allowed the use of P2X7 receptor antagonists in treating spinal cord injury (Peng et al., 2009).

The increase in respiration brought about by ionotropic actions of 1 mM ATP is much larger that caused by 100 μM ATP and is strikingly the same in the presence or absence of extracellular Ca^{2+}, even though there is a large increase in $[Na^+]_I$ in the second, but not the first, condition. As the increase in $[Na^+]_I$ entails a much larger workload than that of $[Ca^{2+}]_I$ (Llorente-Folch et al., 2013), these results suggest that a Ca^{2+}-regulatory boost of mitochondrial respiration in the presence of calcium compensates for the decreased workload in these conditions as compared with a Ca^{2+}-free medium. The players of such Ca^{2+}-regulatory boost may be located in mitochondria, but the participation of the Ca^{2+} regulated mitochondrial transporters of ATP-Mg/Pi SCaMC-3/Slc25a23 (Amigo et al., 2013; Rueda et al., 2015) or Aralar/AGC1/Slc2512 (Juaristi et al., 2017; Llorente-Folch et al., 2013; Llorente-Folch, Rueda, Pérez-Liébana, Satrústegui, & Pardo 2016) in this Ca^{2+}-boost has been ruled out. Further work will be required to clarify the mitochondrial players in this boost. On the other hand, our results show that the Ca^{2+} regulatory boost in respiration may arise from stimulation by 1 mM ATP of a Ca^{2+} dependent increase in glycolytic pyruvate production. Therefore, one important component of the Ca^{2+}-regulatory boost in respiration is increased substrate supply.

Ca^{2+} may have a direct and acute effect on astrocyte glycolysis and pyruvate formation at the level of phosphofructokinase (PFK), by activating the formation of the PFK activator Fructose 2,6-bisphosphate (F2,6BP). Indeed, the bifunctional enzyme responsible for F2,6BP formation in astrocytes is PFKFB3 and it is activated by phosphorylation by AMPK (Almeida, Moncada, & Bolaños, 2004; Bolaños, 2016). In turn, AMPK is regulated allosterically by AMP or ADP and by phosphorylation in α-subunit Thr^{172} by CAMKKβ in response to signals raising intracellular Ca^{2+} (Sanders, Grondin, Hegarty, Snowden, & Carling, 2007; Xiao et al., 2011) as shown in astrocytes (Choi et al., 2017). In sum, stimulation of respiration by 1 mM ATP in the presence of Ca^{2+} in astrocytes involves one or several Ca^{2+}-regulated steps one of which is cytosolic and involves Ca^{2+}-dependent upregulation of glycolysis. Whether glycogen breakdown is also stimulated under these conditions remains to be established. Interestingly, our results show that failure to upregulate

glycolytic pyruvate production by calcium results in an inability to restore the ATP/ADP ratio after agonist addition and in a delayed inability to maintain maximal uncoupled respiration most likely related to the drain in substrate supply.

We find that glutamate or D-aspartate cause an in increase in respiration and in pyruvate formation in astrocytes in a Ca^{2+}-independent way. The nature of the workload induced by glutamate is now well known and is caused by the activation of the Na^+ pump which follows the accumulation of Na^+ within astrocytes that accompanies the transport of the amino acid. The glutamate-induced Na^+ workload was the same in the presence or absence of Ca^{2+} and was directly related with the stimulation of respiration, indicating that the contribution of Ca^{2+} extrusion to this workload is negligible, and that unlike the response to ATP, Ca^{2+} regulation does not play a role in the respiratory response to glutamate. The origin of glutamate-stimulated pyruvate formation is glycolysis from glucose or glycogen, as it is blocked by glycolysis inhibitor (IAA) and enhanced by inhibiting pyruvate/lactate efflux on MCTs (results not shown), but also arises from glutamate metabolism itself, as it is partially resistant to IAA. This is consistent with *in vivo* results indicating that glutamate is partially oxidized in astrocytes and gives rise to pyruvate which may be fully oxidized in astrocytes or rather escape the brain in the form of lactate (Dienel & McKenna, 2014; Hertz et al., 2007; Sonnewald, 2014).

Recent results from the Barros' group have shown that neurons control astrocytic respiration by releasing K^+ and glutamate (Fernández-Moncada et al., 2018). The effects of glutamate and K^+ in astrocyte mitochondria have been also studied recently (Rimmele et al., 2018). K^+ uptake by brain astrocytes or astrocytes in culture resulted in an increase in cytosolic ATP, whereas glutamate uptake caused the reverse effect. The increase in cytosolic ATP caused by K^+ was attributed to an increase in glycolysis followed by an inhibition of respiration explained by a variant of the Crabtree effect in which excess ATP/ADP ratio inhibits OXPHOS. However, the increase in ATP brought about by K^+ is paradoxical given that K^+ removal by astrocytes entails an important workload due to the operation of the Na^+ pump. It is explained by the uptake of bicarbonate through NBCe1 which follows astrocyte K^+-depolarization and causes cytosolic alkalinization and stimulation of glycolysis to increase ATP beyond its use by the Na^+ pump (Bittner et al., 2011; Fernández-Moncada et al., 2018; Rimmele et al., 2018; Theparambil et al., 2014).

We now find that glutamate or D-aspartate, which also stimulate glycolysis, do so with an almost immediate drop on the ATP/ADP ratio. This drop is likely caused by the large workload induced by amino acid uptake causing an immediate ATP demand and a rapid increase in glycolysis and cytosolic pyruvate formation, fueling mitochondria. As a result, ATP levels are rapidly restored. It is likely that respiration and OXPHOS are enhanced by glutamate rather than inhibited, as caused by K^+, due to the lack of ATP accumulation, that is, the lack of Crabtree effect (Fernández-Moncada et al., 2018). It should be noted that at the glutamate concentrations used in this study, the increase in pyruvate formation is immediate suggesting an immediate rather than delayed glutamate-stimulation of glycolysis (Bittner et al., 2011). Interestingly, the rapid upregulation of glycolysis by glutamate/D-aspartate takes place even if, in contrast to K^+ effects, cytosolic pH slightly falls (Figure 8 and Rimmele et al., 2018) which blocks rather than increases glycolysis (Theparambil, Weber, Schmälzle, Ruminot, & Deitmer, 2016) and in the absence of Ca^{2+} signals which may activate CAMKKβ-AMPK-PFKFB3 pathway. It is likely that the extremely rapid fall in ATP/ADP ratio, in itself a potent regulator of glycolysis at various steps, and an AMPK-PFKFB3 activator, is involved in this increase. A role of the AMPK-PFKFB3 pathway for glutamate-stimulation of glycolysis in astrocytes has been

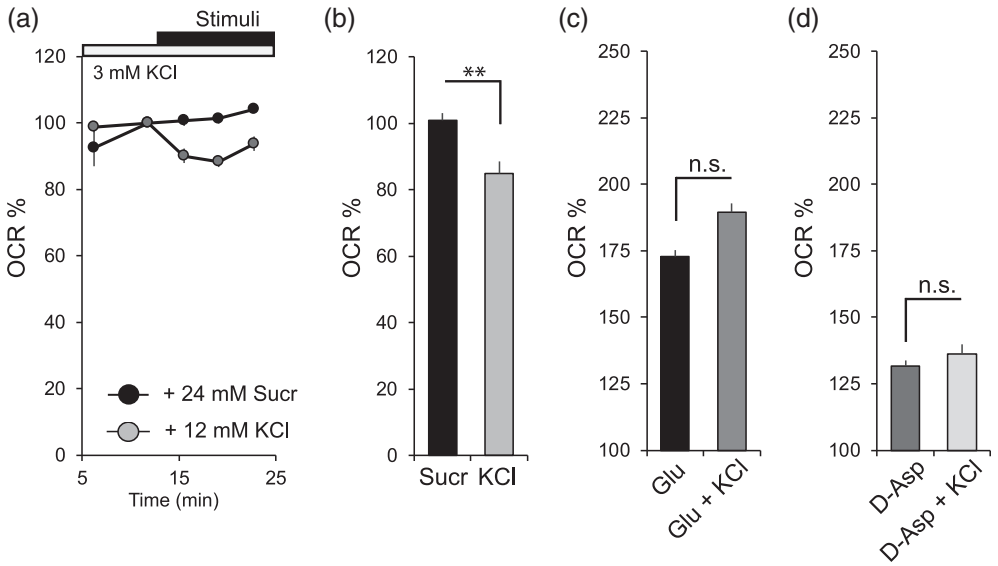

FIGURE 8 Effects of high K^+ and glutamate on mitochondrial respiration. (a) OCR expressed as percentage of basal values in 3 mM KCl media, addition of 12 mM KCl (gray) or 24 mM sucrose (Sucr) (black). (b) KCl induced OCR inhibition from basal values after 3 min of addition normalized without nonmitochondrial values. Data are means ± *SEM* of 6–8 wells from two independent experiments. (c,d) Increase in OCR after 3 min addition of 200 μM glutamate or D-aspartate (500 μM), in 3 mM KCl, or together with the addition of 12 mM KCl. Values normalized from basal OCR without nonmitochondrial OCR. Data are means ± *SEM* from 6 wells from two independent experiments. Means were compared with one-way ANOVA (** $p < .01$)

proposed previously (Ronnett, Ramamurthy, Kleman, Landree, & Aja, 2009).

Taken together, our results indicate that in response to extracellular ATP and glutamate, astrocytes upregulate glycolysis and lactate production, but also pyruvate production and utilization in mitochondria by respiration. The increase in respiration caused by 1 mM ATP and 200 μM glutamate are similar, but ATP does not stimulate cytosolic pyruvate production as much as glutamate. This suggests that a Ca^{2+} regulatory boost of respiration adds to the effects of Ca^{2+} in stimulating glycolytic pyruvate production in providing the full metabolic response to ATP.

K^+ and glutamate, which have opposite effects on astrocyte respiration, flow together in the extracellular space during brain activation and we find that at the glutamate concentrations used, glutamate overcomes the inhibition of respiration caused by high K^+. The high K^+-dependent inhibition of astrocyte respiration is thought to spare oxygen for nearby active neurons, and as K^+ reaches a larger distribution area than the neurotransmitter glutamate, it may provide more oxygen to neurons away from the active zones (Fernández-Moncada et al., 2018). However, in the immediate active regions, glutamate may overcome K^+-respiratory inhibition and astrocytes may employ respiration fueled by glycolytic pyruvate as an additional means to produce ATP in response to the high energy demands. The relative contribution of glutamate activation and high K^+ inhibition of astrocyte respiration and its impact on oxygen supply to neurons will depend on their relative levels (glutamate varying from about 0.02 to 30 μM within the extracellular space to 1 mM in the synaptic cleft following action potential (Moussawi, Riegel, Nair, & Kalivas, 2011), with high glutamate concentrations favoring astrocyte respiration. In addition, the simultaneous presence of high ATP concentrations which also increase astrocyte respiration may further jeopardize oxygen supply to neurons. Understanding these interactions in the brain and is an open question.

ACKNOWLEDGMENTS

This work was supported by grants from Ministerio de Economía SAF2014-56929R (to JS) and SAF2017-82560-R (to AdelA), Fundación Ramón Areces (to JS), Centro de Investigación Biomédica en Red de Enfermedades Raras an initiative of the Instituto de Salud Carlos III (ISCIII), and by an institutional grant from the Fundación Ramón Areces to the Centro de Biología Molecular Severo Ochoa. IJ is recipient of Programa Predoctoral de Formación de Personal Investigador No Doctor from the Departamento de Educación, Política Lingüística y Cultura del Gobierno Vasco. The authors thank Isabel Manso and Bárbara Sesé for technical support and the unit of Optical and Confocal Microscopy of the CBMSO for their support.

CONFLICT OF INTEREST

The authors declare that they have no conflicts of interest.

ORCID

Jorgina Satrústegui https://orcid.org/0000-0003-3377-2667

REFERENCES

Almeida, A., Moncada, S., & Bolaños, J. P. (2004). Nitric oxide switches on glycolysis through the AMP protein kinase and 6-phosphofructo-2-kinase pathway. *Nature Cell Biology*, *6*, 45–51.

Amigo, I., Traba, J., González-Barroso, M. M., Rueda, C. B., Fernández, M., Rial, E., … Del Arco, A. (2013). Glucagon regulation of oxidative phosphorylation requires an increase in matrix adenine nucleotide content through Ca2+ activation of the mitochondrial ATP-mg/pi carrier SCaMC-3. *The Journal of Biological Chemistry*, *288*, 7791–7802.

Attwell, D., & Laughlin, S. B. (2001). An energy budget for signaling in the grey matter of the brain. *Journal of Cerebral Blood Flow and Metabolism*, *21*, 1133–1145.

Azarias, G., Perreten, H., Lengacher, S., Poburko, D., Demaurex, N., Magistretti, P. J., & Chatton, J. Y. (2011). Glutamate transport decreases mitochondrial pH and modulates oxidative metabolism in astrocytes. *The Journal of Neuroscience*, *31*, 3550–3559.

Bittner, C. X., Valdebenito, R., Ruminot, I., Loaiza, A., Larenas, V., Sotelo-Hitschfeld, T., … Barros, L. F. (2011). Fast and reversible stimulation of astrocytic glycolysis by K+ and a delayed and persistent effect of glutamate. *The Journal of Neuroscience*, *31*, 4709–4713.

Bolaños, J. P. (2016). Bioenergetics and redox adaptations of astrocytes to neuronal activity. *Journal of Neurochemistry*, *139*(Suppl 2), 115–125.

Brand, M. D., & Nicholls, D. G. (2011). Assessing mitochondrial dysfunction in cells. *The Biochemical Journal*, *435*, 297–312.

Cahoy, J. D., Emery, B., Kaushal, A., Foo, L. C., Zamanian, J. L., Christopherson, K. S., … Barres, B. A. (2008). A transcriptome database for astrocytes, neurons, and oligodendrocytes: A new resource for understanding brain development and function. *The Journal of Neuroscience*, *28*, 264–278.

Canul-Tec, J. C., Assal, R., Cirri, E., Legrand, P., Brier, S., Chamot-Rooke, J., & Reyes, N. (2017). Structure and allosteric inhibition of excitatory amino acid transporter 1. *Nature*, *544*, 446–451.

Choi, Y. K., Kim, J. H., Lee, D. K., Lee, K. S., Won, M. H., Jeoung, D., … Kim, Y. M. (2017). Carbon monoxide potentiation of L-type Ca2+ channel activity increases HIF-1α-independent VEGF expression via an AMPKα/SIRT1-mediated PGC-1α/ERRα Axis. *Antioxidants & Redox Signaling*, *27*, 21–36.

Covelo, A., & Araque, A. (2018). Neuronal activity determines distinct gliotransmitter release from a single astrocyte. *eLife*, *7*, e32237.

Del Arco, A., & Satrústegui, J. (2004). Identification of a novel human subfamily of mitochondrial carriers with calcium-binding domains. *The Journal of Biological Chemistry*, *279*, 24701–24713.

Dienel, G. A. (2013). Astrocytic energetics during excitatory neurotransmission: What are contributions of glutamate oxidation and glycolysis? *Neurochemistry International*, *63*, 244–258.

Dienel, G. A., & McKenna, M. C. (2014). A dogma-breaking concept: Glutamate oxidation in astrocytes is the source of lactate during aerobic glycolysis in resting subjects. *Journal of Neurochemistry*, *131*, 395–398.

Dienel, G. A., & Cruz, N. F. (2016). Aerobic glycolysis during brain activation: Adrenergic regulation and influence of norepinephrine on astrocytic metabolism. *Journal of Neurochemistry*, *138*, 14–52.

Fernández-Moncada, I., & Barros, L. F. (2014). Non-preferential fuelling of the Na(+)/K(+)-ATPase pump. *The Biochemical Journal*, *460*, 353–361.

Fernández-Moncada, I., Ruminot, I., Robles-Maldonado, D., Alegría, K., Deitmer, J. W., & Barros, L. F. (2018). Neuronal control of astrocytic respiration through a variant of the Crabtree effect. *Proceedings of the National Academy of Sciences of the United States of America*, *115*, 1623–1628.

Fiermonte, G., De Leonardis, F., Todisco, S., Palmieri, L., Lasorsa, F. M., & Palmieri, F. (2004). Identification of the mitochondrial ATP-mg/pi transporter: Bacterial expression, reconstitution, functional characterization, and tissue distribution. *The Journal of Biological Chemistry*, *279*, 30722–30730.

Franke, H., Verkhratsky, A., Burnstock, G., & Illes, P. (2012). Pathophysiology of astroglial purinergic signalling. *Purinergic Signal*, *8*, 629–657.

Gegelashvili, G., & Schousboe, A. (1998). Cellular distribution and kinetic properties of high-affinity glutamate transporters. *Brain Research Bulletin*, *45*(3), 233–238.

Glancy, B., & Balaban, R. S. (2012). Role of mitochondrial Ca2+ in the regulation of cellular energetics. *Biochemistry*, *51*, 2959–2973.

Glancy, B., Willis, W. T., Chess, D. J., & Balaban, R. S. (2013). Effect of calcium on the oxidative phosphorylation cascade in skeletal muscle mitochondria. *Biochemistry*, *52*, 2793–2809.

González-Sánchez, P., Pla-Martín, D., Martínez-Valero, P., Rueda, C. B., Calpena, E., Del Arco, A., … Satrústegui, J. (2017). CMT-linked loss-of-function mutations in GDAP1 impair store-operated Ca2+ entry-stimulated respiration. *Scientific Reports*, *7*, 42993.

González-Sánchez, P., Del Arco, A., Esteban, J. A., & Satrústegui, J. (2017). Store-operated calcium entry is required for mGluR-dependent long term depression in cortical neurons. *Frontiers in Cellular Neuroscience*, *11*, 363.

Grygorowicz, T., Wełniak-Kamińska, M., & Strużyńska, L. (2016). Early P2X7R-related astrogliosis in autoimmune encephalomyelitis. *Molecular and Cellular Neurosciences*, *74*, 1–9.

Hertz, L., & Hertz, E. (2003). Cataplerotic TCA cycle flux determined as glutamate-sustained oxygen consumption in primary cultures of astrocytes. *Neurochemistry International*, *43*, 355–361.

Hertz, L., Peng, L., & Dienel, G. A. (2007). Energy metabolism in astrocytes: High rate of oxidative metabolism and spatiotemporal dependence on glycolysis/glycogenolysis. *Journal of Cerebral Blood Flow and Metabolism*, *27*, 219–249.

Hertz, L., Xu, J., Song, D., Du, T., Li, B., Yan, E., & Peng, L. (2015). Astrocytic glycogenolysis: Mechanisms and functions. *Metabolic Brain Disease*, *30*, 317–333.

Jackson, J. G., O'Donnell, J. C., Takano, H., Coulter, D. A., & Robinson, M. B. (2014). Neuronal activity and glutamate uptake decrease mitochondrial mobility in astrocytes and position mitochondria near glutamate transporters. *The Journal of Neuroscience*, *34*, 1613–1624.

Jackson, J. G., & Robinson, M. B. (2018). Regulation of mitochondrial dynamics in astrocytes: Mechanisms, consequences, and unknowns. *Glia*, *66*, 1213–1234.

Jalil, M. A., Begum, L., Contreras, L., Pardo, B., Iijima, M., Li, M. X., … Saheki, T. (2005). Reduced N-acetylaspartate levels in mice lacking aralar, a brain- and muscle-type mitochondrial aspartate-glutamate carrier. *The Journal of Biological Chemistry*, *280*, 31333–31339.

Jimenez-Blasco, D., Santofimia-Castaño, P., Gonzalez, A., Almeida, A., & Bolaños, J. P. (2015). Astrocyte NMDA receptors' activity sustains neuronal survival through a Cdk5-Nrf2 pathway. *Cell Death and Differentiation*, *22*, 1877–1889.

Juaristi, I., García-Martín, M. L., Rodrigues, T. B., Satrústegui, J., Llorente-Folch, I., & Pardo, B. (2017). ARALAR/AGC1 deficiency, a neurodevelopmental disorder with severe impairment of neuronal mitochondrial respiration, does not produce a primary increase in brain lactate. *Journal of Neurochemistry*, *142*, 132–139.

Kanai, Y., Clémençon, B., Simonin, A., Leuenberger, M., Lochner, M., Weisstanner, M., & Hediger, M. A. (2013). The SLC1 high-affinity glutamate and neutral amino acid transporter family. *Molecular Aspects of Medicine*, *34*, 108–120.

Kirischuk, S., Moller, T., Voitenko, N., Kettenmann, H., & Verkhratsky, A. (1995). ATP-induced cytoplasmic calcium mobilization in Bergmann glial cells. *The Journal of Neuroscience*, *15*, 7861–7871.

Kirischuk, S., Parpura, V., & Verkhratsky, A. (2012). Sodium dynamics: Another key to astroglial excitability? *Trends in Neurosciences*, *35*, 497–506.

Llorente-Folch, I., Rueda, C. B., Amigo, I., del Arco, A., Saheki, T., Pardo, B., & Satrústegui, J. (2013). Calcium-regulation of mitochondrial respiration maintains ATP homeostasis and requires ARALAR/AGC1-malate aspartate shuttle in intact cortical neurons. *The Journal of Neuroscience*, *33*, 13957–13971.

Llorente-Folch, I., Rueda, C. B., Pardo, B., Szabadkai, G., Duchen, M. R., & Satrustegui, J. (2015). The regulation of neuronal mitochondrial metabolism by calcium. *The Journal of Physiology*, *593*, 3447–3462.

Llorente-Folch, I., Rueda, C. B., Pérez-Liébana, I., Satrústegui, J., & Pardo, B. (2016). L-lactate-mediated neuroprotection against glutamate-induced excitotoxicity requires ARALAR/AGC1. *The Journal of Neuroscience*, *36*, 4443–4456.

Lopez-Fabuel, I., Le Douce, J., Logan, A., James, A. M., Bonvento, G., Murphy, M. P., … Bolaños, J. P. (2016). Complex I assembly into supercomplexes determines differential mitochondrial ROS production in neurons and astrocytes. *Proceedings of the National Academy of Sciences of the United States of America*, *113*, 13063–13068.

Lovatt, D., Sonnewald, U., Waagepetersen, H. S., Schousboe, A., He, W., Lin, J. H., … Nedergaard, M. (2007). The transcriptome and metabolic gene signature of protoplasmic astrocytes in the adult murine cortex. *The Journal of Neuroscience*, *27*, 12255–12266.

Magistretti, P. J., & Allaman, I. (2018). Lactate in the brain: From metabolic end-product to signalling molecule. *Nature Reviews. Neuroscience*, *19*, 235–249.

Matute, C. (2011). Glutamate and ATP signalling in white matter pathology. *Journal of Anatomy*, *219*, 53–64.

Martinez-Serrano, A., Blanco, P., & Satrústegui, J. (1992). Calcium binding to the cytosol and calcium extrusion mechanisms in intact synaptosomes and their alterations with aging. *The Journal of Biological Chemistry*, *267*, 4672–4679.

Moussawi, K., Riegel, A., Nair, S., & Kalivas, P. W. (2011). Extracellular glutamate: Functional compartments operate in different concentration ranges. *Frontiers in Systems Neuroscience*, *24*, 1–9.

Müller, M. S., Fox, R., Schousboe, A., Waagepetersen, H. S., & Bak, L. K. (2014). Astrocyte glycogenolysis is triggered by store-operated calcium entry and provides metabolic energy for cellular calcium homeostasis. *Glia*, *62*, 526–534.

Nissen, J. D., Pajecka k, S. M. H., Skytt, D. M., & Waagepetersen, H. S. (2015). Dysfunctional TCA-cycle metabolism in glutamate dehydrogenase deficient astrocytes. *Glia*, *63*, 2313–2326.

Nortley, R., & Attwell, D. (2017). Control of brain energy supply by astrocytes. *Current Opinion in Neurobiology*, *47*, 80–85.

Palmieri, L., Pardo, B., Lasorsa, F. M., del Arco, A., Kobayashi, K., Iijima, M., … Palmieri, F. (2001). Citrin and aralar1 are ca(2+)-stimulated aspartate/glutamate transporters in mitochondria. *The EMBO Journal*, *20*, 5060–5069.

Panatier, A., & Robitaille, R. (2016). Astrocytic mGluR5 and the tripartite synapse. *Neuroscience*, *323*, 29–34.

Pardo, B., Contreras, L., Serrano, A., Ramos, M., Kobayashi, K., Iijima, M., … Satrústegui, J. (2006). Essential role of aralar in the transduction of small Ca2+ signals to neuronal mitochondria. *The Journal of Biological Chemistry*, *281*, 1039–1047.

Parpura, V., Fisher, E. S., Lechleiter, J. D., Schousboe, A., Waagepetersen, H. S., Brunet, S., … Verkhratsky, A. (2017). Glutamate and ATP at the Interface between signaling and metabolism in Astroglia: Examples from pathology. *Neurochemical Research*, *42*, 19–34.

Pellerin, L., & Magistretti, P. J. (1994). Glutamate uptake into astrocytes stimulates aerobic glycolysis: A mechanism coupling neuronal activity to glucose utilization. *Proceedings of the National Academy of Sciences of the United States of America*, *91*, 10625–10629.

Peng, W., Cotrina, M. L., Han, X., Yu, H., Bekar, L., Blum, L., … Nedergaard, M. (2009). Systemic administration of an antagonist of the ATP-sensitive receptor P2X7 improves recovery after spinal cord injury. *Proceedings of the National Academy of Sciences of the United States of America*, *106*, 12489–12493.

Porras, O. H., Ruminot, I., Loaiza, A., & Barros, L. F. (2008). Na(+)-ca(2+) cosignaling in the stimulation of the glucose transporter GLUT1 in cultured astrocytes. *Glia*, *56*, 59–68.

Putney, J. W. (2009). Capacitative calcium entry: From concept to molecules. *Immunological Reviews*, *231*, 10–22.

Rimmele, T. S., de Castro Abrantes, H., Wellbourne-Wood, J., Lengacher, S., & Chatton, J. Y. (2018). Extracellular potassium and glutamate interact to modulate mitochondria in astrocytes. *ACS Chemical Neuroscience*, *9*, 2009–2015.

Rojas, H., Colina, C., Ramos, M., Benaim, G., Jaffe, E. H., Caputo, C., & DiPolo, R. (2007). Na+ entry via glutamate transporter activates the reverse Na+/Ca2+ exchange and triggers ca(i)2+—induced Ca2+ release in rat cerebellar Type-1 astrocytes. *Journal of Neurochemistry*, *100*, 1188–1202.

Ronnett, G. V., Ramamurthy, S., Kleman, A. M., Landree, L. E., & Aja, S. (2009). AMPK in the brain: Its roles in energy balance and neuroprotection. *Journal of Neurochemistry*, *109*(Suppl 1), 17–23.

Rose, C. R., & Ransom, B. R. (1997). Gap junctions equalize intracellular Na + concentration in astrocytes. *Glia*, *20*, 299–307.

Rueda, C. B., Llorente-Folch, I., Amigo, I., Contreras, L., González-Sánchez, P., Martínez-Valero, P., … Satrústegui, J. (2014). Ca(2+)

regulation of mitochondrial function in neurons. *Biochimica et Biophysica Acta*, *1837*, 1617–1624.

Rueda, C. B., Traba, J., Amigo, I., Llorente-Folch, I., González-Sánchez, P., Pardo, B., … Satrústegui, J. (2015). Mitochondrial ATP-mg/pi carrier SCaMC-3/Slc25a23 counteracts PARP-1-dependent fall in mitochondrial ATP caused by excitotoxic insults in neurons. *The Journal of Neuroscience*, *35*, 3566–3581.

Ruiz, F., Alvarez, G., Pereira, R., Hernández, M., Villalba, M., Cruz, F., … Satrústegui, J. (1998). Protection by pyruvate and malate against glutamate-mediated neurotoxicity. *Neuroreport*, *9*, 1277–1282.

Ruminot, I., Schmälzle, J., Leyton, B., Barros, L. F., & Deitmer, J. W. (2017). Tight coupling of astrocyte energy metabolism to synaptic activity revealed by genetically encoded FRET nanosensors in hippocampal tissue. *The Journal of Cerebral Blood Flow & Metabolism*, *1*, 0271678X1773701. https://doi.org/10.1177/0271678X17737012

Salter, M. W., & Hicks, J. L. (1994). ATP-evoked increases in intracellular calcium in neurons and glia from the dorsal spinal cord. *The Journal of Neuroscience*, *14*, 1563–1575.

Salas, E., Carrasquero, L. M., Olivos-Ore, L. A., Bustillo, D., Artalejo, A. R., Miras-Portugal, M. T., & Delicado, E. G. (2013). Purinergic P2X7 receptors mediate cell death in mouse cerebellar astrocytes in culture. *The Journal of Pharmacology and Experimental Therapeutics*, *347*, 802–815.

Sanders, M. J., Grondin, P. O., Hegarty, B. D., Snowden, M. A., & Carling, D. (2007). Investigating the mechanism for AMP activation of the AMP-activated protein kinase cascade. *The Biochemical Journal*, *403*, 139–148.

San Martin, A., Ceballo, S., Baeza-Lehnert, F., Lerchundi, R., Valdebenito, R., Contreras-Baeza, Y., … Barros, L. F. (2014). Imaging mitochondrial flux in single cells with a FRET sensor for pyruvate. *PLoS One*, *9*, e85780.

San Martin, A., Arce-Molina, R., Galaz, A., Pérez-Guerra, G., & Barros, L. F. (2017). Nanomolar nitric oxide concentrations quickly and reversibly modulate astrocytic energy metabolism. *The Journal of Biological Chemistry*, *292*, 9432–9438.

Satrústegui, J., Pardo, B., & Del Arco, A. (2007). Mitochondrial transporters as novel targets for intracellular calcium signaling. *Physiological Reviews*, *87*, 29–67.

Sharma, K., Schmitt, S., Bergner, C. G., Tyanova, S., Kannaiyan, N., Manrique-Hoyos, N., … Simons, M. (2015). Cell type- and brain region-resolved mouse brain proteome. *Nature Neuroscience*, *18*, 1819–1831.

Shen, W., Nikolic, L., Meunier, C., Pfrieger, F., & Audinat, E. (2017). An autocrine purinergic signaling controls astrocyte-induced neuronal excitation. *Scientific Reports*, *7*, 11280.

Silver, I. A., & Erecińska, M. (1994). Extracellular glucose concentration in mammalian brain: Continuous monitoring of changes during increased neuronal activity and upon limitation in oxygen supply in normo-, hypo-, and hyperglycemic animals. *The Journal of Neuroscience*, *14*, 5068–5076.

Sonnewald, U. (2014). Glutamate synthesis has to be matched by its degradation - where do all the carbons go? *Journal of Neurochemistry*, *131*, 399–406.

Stephen, T. L., Higgs, N. F., Sheehan, D. F., Al Awabdh, S., Lopez-Domenech, G., Arancibia-Carcamo, I. L., & Kittler, J. T. (2015). Miro1 regulates activity-driven positioning of mitochondria within astrocytic processes apposed to synapses to regulate intracellular calcium signaling. *The Journal of Neuroscience*, *35*, 15996–16011.

Sun, W., McConnell, E., Pare, J. F., Xu, Q., Chen, M., Peng, W., … Nedergaard, M. (2013). Glutamate-dependent neuroglial calcium signaling differs between young and adult brain. *Science*, *339*, 197–200.

Supplie, L. M., Düking, T., Campbell, G., Diaz, F., Moraes, C. T., Götz, M., … Nave, K. A. (2017). Respiration-deficient astrocytes survive as glycolytic cells in vivo. *The Journal of Neuroscience*, *37*, 4231–4242.

Tantama, M., Martínez-Francois, J. R., Mongeon, R., & Yellen, G. (2013). Imaging energy status in live cells with a fluorescent biosensor of the intracellular ATP-to-ADP ratio. *Nature Communications*, *4*, 2550.

Theparambil, S. M., Ruminot, I., Schneider, H. P., Shull, G. E., & Deitmer, J. W. (2014). The electrogenic sodium bicarbonate cotransporter NBCe1 is a high-affinity bicarbonate carrier in cortical astrocytes. *The Journal of Neuroscience*, *34*, 1148–1157.

Theparambil, S. M., Weber, T., Schmälzle, J., Ruminot, I., & Deitmer, J. W. (2016). Proton fall or bicarbonate rise: Glycolytic rate in mouse astrocytes is paved by intracellular alkalinization. *The Journal of Biological Chemistry*, *291*, 19108–19117.

Verkhratsky, A., Orkand, R. K., & Kettenmann, H. (1998). Glial calcium: Homeostasis and signaling function. *Physiological Reviews*, *78*, 99–141.

Verkhratsky, A., Krishtal, O. A., & Burnstock, G. (2009). Purinoceptors on neuroglia. *Molecular Neurobiology*, *39*, 190–208.

Wong-Riley, M. T., Trusk, T. C., Tripathi, S. C., & Hoppe, D. A. (1989). Effect of retinal impulse blockage on cytochrome oxidase-rich zones in the macaque striate cortex: II. Quantitative electron-microscopic (EM) analysis of neuropil. *Visual Neuroscience*, *2*, 499–514.

Xiao, B., Sanders, M. J., Underwood, E., Heath, R., Mayer, F. V., Carmena, D., … Gamblin, S. J. (2011). Structure of mammalian AMPK and its regulation by ADP. *Nature*, *472*, 230–233.

How to cite this article: Juaristi I, Llorente-Folch I, Satrústegui J, del Arco A. Extracellular ATP and glutamate drive pyruvate production and energy demand to regulate mitochondrial respiration in astrocytes. *Glia*. 2019;67: 759–774. https://doi.org/10.1002/glia.23574